Physica Scripta

PAPER

Cosmological redshift from translations in an Einstein-Milne universe relativity with bounded position and velocity

Kamal Hajian *

Institute of Physics, University of Oldenburg, D-26111 Oldenburg, Germany

* Author to whom any correspondence should be addressed.

E-mail: kamal.hajian@uni-oldenburg.de

Keywords: cosmological constant, Milne model, special relativity, general relativity, center manifold theory, cosmological redshift, Hubble tension

OPEN ACCESS

RECEIVED
6 May 2025

REVISED
11 July 2025

ACCEPTED FOR PUBLICATION
17 July 2025

PUBLISHED
29 July 2025

Abstract

Milne Universe is one of the models of cosmology that employs hyperboloids as its surfaces of constant time. The special relativistic construction of the model, though very interesting, has problems with the observational data. We suggest a method to modify the model and remedy its issues. The idea is to change the coordinates of the observers from the origin to a distance d in the time direction. It is similar to the velocity 4-vector that does not vanish for an observer at rest and has a component c in the timelike direction. The constant d is an invariant length that acts as a bound for position in the same way that c serves as a bound for velocity. In this regard, translations in space turn out to be boosts, similar to the translations in velocity. In this model, which we call Einstein-Milne, the cosmological redshift is a result of spatial translations via the Doppler effect. We show that the model can explain the Hubble diagram without assuming dark matter and energy, as well as acceleration of the Universe. The Hubble constant is obtained as a function of supernovae Ia absolute magnitude by fitting the predicted Hubble diagram to the data, which provides a means of releasing its tension.

1. Introduction

Edwin Hubble's discovery of non-zero receding velocity of galaxies that is linear in distances has revolutionized our understanding of the Universe [1]. About a century after his discovery, the Hubble constant H_0 is still the most important parameter in cosmology. The abundance of observational data in the last decades has increased the accuracy of this constant in gravitational models. In addition, the data, specially from the Supernova Cosmology Project [2], the High-Z Supernova Search Team on Type Ia supernovae (SNe Ia) [3], and the Low-Z Caĺan/Tololo observations [4–6], has shed light on the dynamics of the Universe as it expands (Rev. [7]). Such data is extended in numbers by Dark Energy Survey (DES) program [8–14] and other projects (e.g., CfA [15, 16], CNIa [17], and others [18–20]) with improvements of search algorithms and analyses (e.g., as in [21–24]) while in parallel, theoretical physicists try to confirm or modify the existing cosmological models or develop new ones. The most successful model in explaining the observations, so far, has been the ΛCDM [25–27], that is a Friedmann-Lemaître-Robertson-Walker (FLRW) metric in general relativity (GR) with roughly 70% dark energy in the form of cosmological constant Λ [28], 25% (cold) dark matter (Revs. [29, 30]), and 5% ordinary matter (e.g., see [31]).

In spite of the splendid success of the ΛCDM in explanation of the cosmological data and acceleration of the Universe (Rev. [32]), there are some challenges with this model (Revs. [33–35]). One of the issues that is relevant to our discussion is the amount of hypothetical entities in the model, namely the dark sector. That is, after decades of investigations, there is not yet a convincing non-gravitational explanation or evidence for dark energy and matter. On top of this dilemma, recent observations of high redshift quasars [36], gamma ray bursts (GRB) [37, 38], and SNe [8–14] have implied a mismatch between the amount of the best fitting dark energy and matter in comparison with the similar parameters that could be deduced from the earlier observations mentioned above (e.g., GRB and quasars in [39, 40] and SNe in [41–47]). Another important issue related to the analysis of

this paper is the Hubble tension. Based on the predictions of the ΛCDM model from the SN Ia observations, H_0 turns out to have a value of $73.30 \pm 1.04 \mathrm{kms}^{-1}\mathrm{Mpc}^{-1}$ [48] (see also other reports in [23, 49–55] with values around this number). On the other hand, Planck observations of the cosmic microwave background (CMB) anisotropies have resulted in $67.4 \pm 0.5 \mathrm{kms}^{-1}\mathrm{Mpc}^{-1}$ [31, 56] (see the results in [57–61] in agreement with this value). The two values of H_0 are about 4σ discrepant, which is known as the Hubble tension (Revs. [33, 62, 63]).

There are analyses in the literature (e.g., [64, 65]) to show that some of the problems are resolvable without necessity of modification of the gravitational theory. On the other side, there are proposals for modification of the gravitational model to overcome the issues. A non-exclusive list of such approaches can be found in [63, 66, 67].

One of the proposals to deal with the expansion of the Universe is the Milne model [68–70] (Revs. [71, 72]). The aim of this model is to provide an explanation for the recession velocities of galaxies solely based on special relativity. The mathematical structure of the model is based on the hyperboloid foliation of the Minkowski spacetime. An easy way to understand the Milne model is to focus on the FLRW coordination of the Minkowski spacetime. To have a self-contained introduction and fix the notation, we briefly review the model here.

Milne model: a brief review

The Minknowski geometry in Cartesian coordinates $X^\mu = (cT, X, Y, Z)$ is

$$\mathrm{d}s^2 = -c^2\mathrm{d}T^2 + \mathrm{d}X^2 + \mathrm{d}Y^2 + \mathrm{d}Z^2, \tag{1}$$

which in spherical coordinates $X^\mu_s = (cT,\ R,\ \theta,\ \varphi)$ would be

$$X = R\sin\theta\cos\varphi, \qquad Y = R\sin\theta\sin\varphi, \qquad Z = R\cos\theta, \tag{2}$$

$$\mathrm{d}s^2 = -c^2\mathrm{d}T^2 + \mathrm{d}R^2 + R^2(\mathrm{d}\theta^2 + \sin^2\theta\mathrm{d}\varphi^2). \tag{3}$$

It is possible to change from the spherical to the Milne coordinates $(\tau, \chi, \theta, \varphi)$

$$T = \tau\cosh\chi, \qquad R = c\tau\sinh\chi, \tag{4}$$

$$\mathrm{d}s^2 = -c^2\mathrm{d}\tau^2 + c^2\tau^2(\mathrm{d}\chi^2 + \sinh^2\chi(\mathrm{d}\theta^2 + \sin^2\theta\mathrm{d}\varphi^2)). \tag{5}$$

Introducing the new radial coordinate $\bar{R} = \sinh\chi$, the metric can be re-written as a FLRW metric

$$\mathrm{d}s^2 = -c^2\mathrm{d}\tau^2 + a^2(\tau)\left(\frac{\mathrm{d}\bar{R}^2}{1 - k\bar{R}^2} + \bar{R}^2(\mathrm{d}\theta^2 + \sin^2\theta\mathrm{d}\varphi^2)\right) \tag{6}$$

with $k = -1$ and $a(\tau) = c\tau$. In this coordinate, the surfaces of constant τ have the constant negative curvature. To see this, by calculation of their extrinsic metric $K_{\mu\nu}$ we find

$$K = K^\alpha{}_\alpha = \frac{-3\frac{\mathrm{d}a(\tau)}{\mathrm{d}\tau}}{ca(\tau)} = \frac{-3}{c\tau}. \tag{7}$$

As a result, the mean curvature of these surfaces is $\frac{K}{3} = \frac{-1}{c\tau}$. Moreover, the three dimensional Ricci scalar of them is found to be equal to $\frac{-6}{c^2\tau^2}$ that is a negative constant for a fixed τ. So, they are hyperbolic 3-spaces, $\mathbb{H}^3$, also called two-sheeted hyperboloid of revolution, that we call them hyperboloids for short. These maximally symmetric hypersurfaces are known since the 19th century by great mathematicians such as Gauss, Lobachevsky, and Bolyai (Rev. [73]). The Milne metric in equation (6) is a coordinate representation of the flat, four-dimensional Minkowski geometry that is maximally symmetric and possesses rotations, boosts, and translations as its isometries.

We note that at $\tau \to 0$ there is a coordinate singularity in the Milne metric. Nonetheless, in his model an initial condition is imposed at this singular point $\tau = T = R = 0$, and it is assumed that a random initial velocity distribution yields the galaxies move on the straight worldlines of constant $\bar{R}$ forever, i.e., they reside at a constant comoving radius $\bar{R}$, and hence, constant χ. In this way, by equation (4), their radial velocity is

$$v_H = \frac{\mathrm{d}R}{\mathrm{d}T} = c\tanh\chi = \frac{R}{T}. \tag{8}$$

Denoting the inverse of the current age of the Universe by H_0, then at present, i.e., at $T = \frac{1}{H_0}$,

$$v_H|_{\text{present}} = H_0 R = \frac{H_0 R_e}{1 - \frac{H_0 R_e}{c}}, \qquad R_e = \frac{R}{1 + \frac{H_0 R}{c}}, \tag{9}$$

that is Hubble's law in Milne model. The R_e denotes the radial coordinate of the Galaxy at the time of emission of its light ray towards us, and its relation with the R can be found by simple trigonometry. The radial velocity v_H implies a redshift in the spectrum of the observed galaxies because of the special relativistic Doppler effect. Notice that the Hubble constant H_0 is not a fundamental constant in the Milne model and is simply the age of the

Universe in which we live at the present. For the observers in the past and future, H_0 takes the inverse value of their cosmic time as the proportionality coefficient in equation (9).

In spite of the simplicity and elegance of the Milne model, it has some theoretical and observational challenges to deal with. Although the distribution of matter is homogeneous and isotropic on the hyperboloids of constant τ, it is not clear why the matter has exploded from a point of space, that is, $R=0$, where we are living. In other words, what is the reason for such discrimination between us and other distant observers in our special relativistic inertial frame, i.e., those who are at rest w.r.t us? It is regrettable that they will not be able to observe the isotropic cosmic redshift because the Universe has not exploded from their position if they follow their worldline back in time. The answer to this fundamental question is not straightforward in the Milne model. Another challenge is with the dynamics of the metric. The Milne metric in (5) is a member of FLRW metrics that, by the Einstein equations, is expected to satisfy the Friedmann equations

$$\left(\frac{\dot{a}}{a}\right)^2+\frac{kc^2}{a^2}=\frac{8\pi G}{3}\rho+\frac{\Lambda c^2}{3},\ \frac{\ddot{a}}{a}=\frac{-4\pi G}{3}\left(\rho+\frac{3P}{c^2}\right)+\frac{\Lambda c^2}{3}\,, \tag{10}$$

in which the dot denotes derivation with respect to τ. The symbols Λ, ρ and P denote the cosmological constant, the energy density and pressure of the matter as a perfect fluid (including radiation, baryons, and dark matter), respectively. Noting that the Milne metric is the Minkowski metric, the r.h.s of the (10) has to vanish because the Minkowski is a vacuum solution. However, for a FLRW metric with GR dynamics, the observed data of the redshift and luminosity distances imposes constraints on the values of ρ, P, and Λ. In this context, the data is in favor of non-vanishing values for these quantities, indicating the necessity of dark matter and dark energy. Moreover, the best fit for the k turns out to be close to zero, that is in contrast with the $k=-1$ in Milne's model. Saying in another words, the Milne model fails to reproduce the Hubble diagram of the observed distance celestial objects (see [74–77]). In this regard, one can conclude that the Milne model is falsified by the observation. It may be the reason that this model is not in the streamline of the cosmological investigations. Nonetheless, the reader may be interested in looking at the works that study different aspects of the model, e.g., in [78–90], and alternatives to this model listed in e.g., [63, 66, 67].

Interestingly, it is possible to open a new way to deal with the challenges of the Milne and ΛCDM models. The idea is to introduce the Hubble constant via a fundamental constant similar to the speed of light c. This new constant, denoted by d, is a dimensionful constant with the dimensions of length. In parallel to c that delimits velocities in the Minkowski spacetime, d delimits the 'position.' The d is introduced such that it is an invariant bound, similar to c that is an invariant maximum speed, i.e., they have the same value for all inertial observers. Surprisingly, such a modification can remedy the issues mentioned above and construct a new setup in the context of large-scale gravitational formulations. To this end, in the rest of the paper we seldom refer to the Milne coordinates. Instead, another coordinate is employed that is more suitable for such a modification; that can be called the Einstein-Milne (EM) coordinate.

The paper is organized as follows: In the next section, inertial observers and frames in special relativity are reviewed for later discussions. In section 3, the EM coordinates and frames are introduced. Transformations within and between EM frames and their implications are studied in section 4. In section 5 we explain how the EM model resolves the 'center' from the Milne universe. The GR dynamics of the model is investigated in section 6. Theoretical prediction of the model for the Hubble diagram and its agreement with the observational data are presented in section 7. In the last section, that is section 8, some clarifying discussions, the outlook of the formulation for future works, and the conclusion are provided.

2. Review: Minkowski in cartesian coordinates

This section, although it may look very elementary (and probably boring) to an expert, is important in fully understanding the upcoming sections. It is a purposeful review of the Minkowski spacetime in four dimensions with signature $(-1,1,1,1)$. The Greek indices run from 0 to 3 in accordance with the signature. We will keep the speed of light c, Newton constant G, and Planck constant $\hbar$ explicit. The function $\log(\dots)$ is the logarithm with base 10, and $\ln(\dots)$ denotes the natural logarithm.

2.1. Cartesian coordinates

Beginning from the metric in Cartesian coordinates (1), an event is a point, as illustrated in figure 1, and is specified by a coordinate (cT, X, Y, Z). A classical massive point particle is identified by a timelike line in the geometry; that is its worldline. The velocity of such a particle is given by

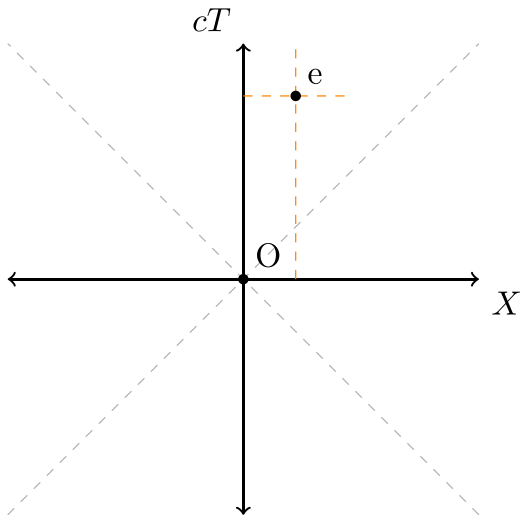

Figure 1. In Cartesian coordinates, the observer O is assumed to be at the origin. An event e is a point that is identified by its coordinates (cT, X, Y, Z). The orange dashed lines show the hypersurfaces of constants T and X. The gray dashed lines show one of the light cones.

$$\begin{cases} u_X = \frac{\mathrm{d}X}{\mathrm{d}T} \\ u_Y = \frac{\mathrm{d}Y}{\mathrm{d}T}, \\ u_Z = \frac{\mathrm{d}Z}{\mathrm{d}T} \end{cases} \quad \overrightarrow{u} \equiv (u_X, u_Y, u_Z),\ u \equiv \sqrt{u_X^2 + u_Y^2 + u_Z^2} \tag{11}$$

and its 4-vector

$$U^\mu = \frac{\mathrm{d}X^\mu}{\mathrm{d}\sigma} = \frac{1}{\sqrt{1 - \frac{u^2}{c^2}}} \begin{pmatrix} c \\ u_X \\ u_Y \\ u_Z \end{pmatrix}, \tag{12}$$

in which the proper time of a moving object is denoted by σ. On the other hand, the light, as well as other massless particles, move on lightlike worldlines, i.e., the lines with $\frac{\pi}{4}$ angle w.r.t the time axis.

2.2. Inertial observers and frames

2.2.1. Inertial observers

The observers that move freely, i.e., on straight worldlines in Minkowski background, are called inertial observers. They have a constant velocity, and as long as the physics in special relativity is concerned, they are equivalent without any preferences among them. The group of transformations among the inertial observers is the celebrated Poincaré group. Let us review these transformations carefully that is appropriate for later discussion. Beginning from the Cartesian coordinate $\tilde{X}^\mu$, we consider two inertial observers, O at $\tilde{X}^\mu_{\mathrm{O}} = (cT_{\mathrm{O}}, X_{\mathrm{O}}, Y_{\mathrm{O}}, Z_{\mathrm{O}})$ and O′ at $\tilde{X}^\mu_{\mathrm{O}'} = (cT_{\mathrm{O}'}, X_{\mathrm{O}'}, Y_{\mathrm{O}'}, Z_{\mathrm{O}'})$. The coordinates that the observers O and O′ attribute to the events can be denoted by X^μ and X'^μ respectively. Assume also that the observer O′ has a relative velocity $\overrightarrow{v}$ as measured by O, that is, when it is measured in the X^μ system of coordinates. By the relativity principle, there is no absolute velocity for the inertial observers, so we can conventionally choose the O to be at rest in the coordinates $\tilde{X}^\mu$.

In addition to the information above, we need two more pieces of information to be able to change from X^μ to X'^μ: the coordinates of the origins of the X^μ and X'^μ systems in the $\tilde{X}^\mu$ system. Let us denote them by $\bar{X}^\mu = (c\bar{T}, \bar{X}, \bar{Y}, \bar{Z})$ and $\bar{X}'^\mu = (c\bar{T}', \bar{X}', \bar{Y}', \bar{Z}')$ respectively. In this setup, the transformations from O to O′ that map the X^μ to X'^μ are

$$X'^\mu = \Lambda^\mu_\nu(\overrightarrow{v})(X^\nu - (\bar{X}'^\nu - \bar{X}^\nu)), \tag{13}$$

in which the $\Lambda^\mu_\nu(\overrightarrow{v})$ is the Lorentz group. In this paper the rotation subgroup is irrelevant and trivial in our discussions, and we seldom mention it in the Lorentz group, while our focus will be on boosts.

It is possible to trim the relation (13) a bit. The auxiliary (or better to say, the redundant) coordinate $\tilde{X}^\mu$ does not appear explicitly in it. Noting that the difference $\bar{X}'^\nu - \bar{X}^\nu$ is the same in $\tilde{X}^\mu$ and X^μ, we could ignore the coordinate $\tilde{X}^\mu$ from the beginning and use the coordinate X^μ. It means that we could begin our analysis directly from the O's coordinate system. The identification $X^\mu = \tilde{X}^\mu$ means that the origin of $\tilde{X}^\mu$ is chosen to be the same as the origin of X^μ, i.e., $\bar{X}^\mu = (0, 0, 0, 0)$. In addition, we notice that the X^μ_{O} and $X^\mu_{\mathrm{O}'}$ do not play any role

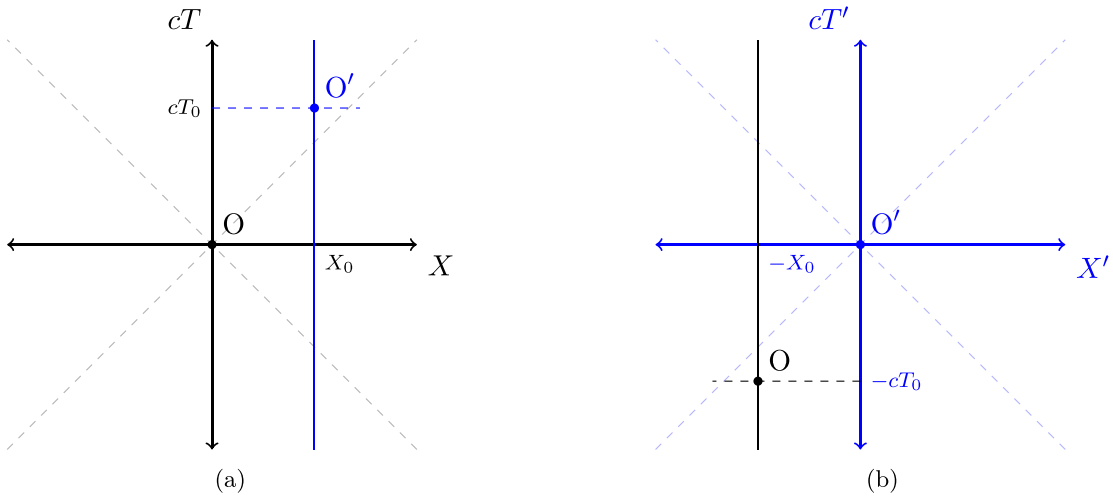

Figure 2. Translations from an observer O to O′ in Cartesian coordinates. (a) From the point of view of O, the observer O′ is situated at (cT_0, X_0) with the worldline depicted by a solid blue line. (b) After the translations, the observer O′ is at the origin, while the observer O is at $(-cT_0, -X_0)$ in primed coordinates and follows the solid black worldline.

in the formula. In order to drop this redundancy too, it is standard (but conventional) to consider the observers at the origin of their coordinates; that means $\bar{X}^\mu = X^\mu_{\rm O}$ and $\bar{X}'^\mu = X^\mu_{\rm O'}$. These identifications, together with the previous one, yield $X^\mu_{\rm O} = (0,\ 0,\ 0,\ 0)$. Considering all of the above in (13), we achieve the standard Poincaré transformation

$$X'^\mu = \Lambda^\mu_\nu(\overrightarrow{v})(X^\nu - X^\nu_{\rm O'}). \tag{14}$$

The term in the parenthesis is the action of the group of translations in space and time, and the $\Lambda^\mu_\nu(\overrightarrow{v})$ is the standard notation of the Lorentz group. By setting $X^\nu = X^\nu_{\rm O'}$ in (14) it is clear that the new observer O′ also attributes the coordinate $X'^\mu_{\rm O'} = (0,\ 0,\ 0,\ 0)$ to himself.

2.2.2. Inertial frames

Another useful concept in the formulation of classical mechanics is the inertial frame. The concept distinguishes the action of translations and boosts in Poincaré group. Translations in space and time in Cartesian coordinates are shifts by a constant vector X^μ_0

$$X'^\mu = X^\mu - X^\mu_0. \tag{15}$$

Conventionally, the observers that are related to each other by the translations (15), as well as the rotations, are considered to be in the same inertial frame (we do not study accelerating observers in this paper). From the physical point of view, the shift in (15) describes a change from the observer O at the origin $X^\mu = (0, 0, 0, 0)$ to an observer O′ that is at rest and situated at the point $X^\mu_0 = (cT_0,\ X_0,\ Y_0,\ Z_0)$. Such a translation is illustration in figure 2.

It is conventional to illustrate the Minkowski spacetime by the two dimensions cT and X and eliminate the coordinates Y and Z. So, the X direction will be the representative of all three spatial dimensions. Besides, this spatial direction is usually chosen to be in the direction of the velocity of the object or observer. In the rest of the paper, we use this convention whenever it is not necessary to consider all three dimensions.

In order to change coordinates for the observers in other inertial frames, special relativity employs a set of transformations that are called boosts. As it was alluded to in the previous section, rotations and boosts constitute a group that is called the Lorentz group. Explicitly and as a simple example, the transformation from the coordinates X^μ of an observer O at the origin $X^\mu_{\rm O} = (0,\ 0,\ 0,\ 0)$ to X'^μ of an observer O′ situated at $X^\mu_{\rm O'} = (cT_0,\ X_0,\ Y_0,\ Z_0)$ and with the velocity v along the X direction is given by (14) in which

$$\Lambda^\mu_\nu(v) = \begin{pmatrix} \gamma & -\gamma\beta & 0 & 0 \\ -\gamma\beta & \gamma & 0 & 0 \\ 0 & 0 & 1 & 0 \\ 0 & 0 & 0 & 1 \end{pmatrix}, \qquad \gamma = \frac{1}{\sqrt{1-\beta^2}}, \qquad \beta = \frac{v}{c}. \tag{16}$$

In summary, the translations and rotations change observers within one inertial frame, and the boosts transform to another inertial frame.

For later arguments, it is important here to emphasize that the boost in $\Lambda^\mu{}_\nu$ has the job of changing (or in the context of this paper, translating) the velocity while not changing the position or clock of the observer (not to be

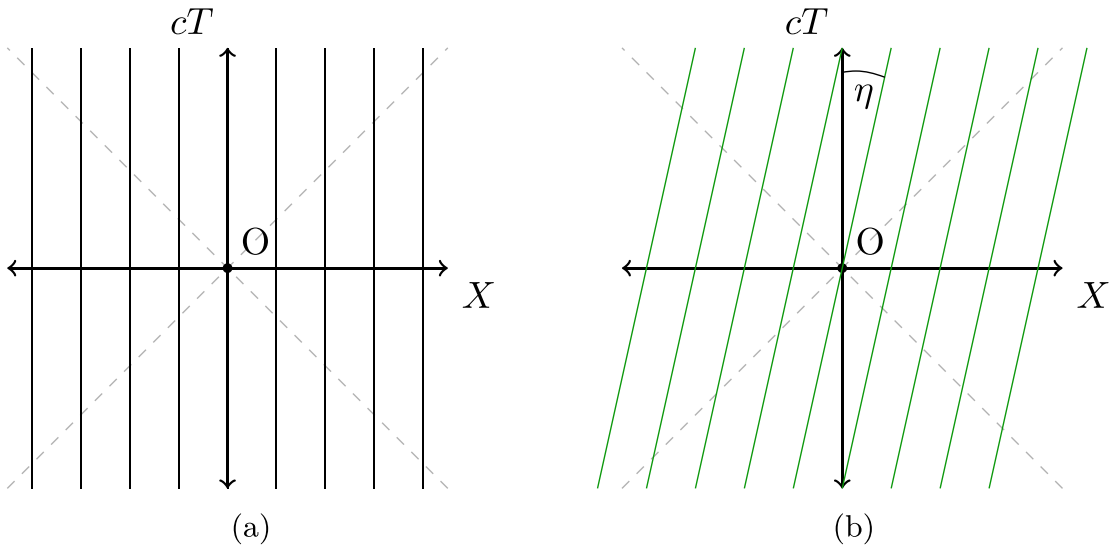

Figure 3. (a) The inertial frame associated with the observer O that can be visualized by the worldlines of all observers that are at rest with respect to her, and (b) another inertial frame that is moving with a relative velocity $v = c \tan\eta$.

confused by her clock rate). It is because, by such a boost, the initial observer coincides at position and time with the new observer. They are at $X^\mu = (0, 0, 0, 0)$ and $X'^\mu = (0,\ 0,\ 0,\ 0)$ respectively, which is the same point in the spacetime. To change the position and clock of an observer, another transformation is used, which are the shifts in space and time in equation (15).

A simple way to visualize an inertial frame is to consider the worldlines of all observers with zero relative velocity, as in figure 3(a). The set of all straight and parallel worldlines with the angle $\eta = \tan^{-1}(|\beta|) \neq 0$ with respect to the cT axis (see figure 3(b)) constitutes another legitimate inertial frame if $\eta < \frac{\pi}{4}$, i.e., the relative velocity that labels the observers is less than the speed of light.

After the elementary review of special relativity, we can start the main part of the paper, which is a modification of the relation between observers and the transformations in special relativity.

3. Minkowski in Einstein-Milne coordinates

In classical mechanics before special relativity, Galilean transformations were used to translate in space and time, as well as changing inertial frames. The latter, i.e., changing the inertial frames, could also be considered as 'translations' in velocities. In both cases, translations in space and time, and velocities, there were not any bounds on the values of translations. One could change the position, time, and velocity as much as she wanted. In special relativity, Einstein kept the translations in space and time intact, while he changed the translations in the velocities such that there would be an upper bound on the velocities, that is, the speed of light c.

The main idea of this section is to modify translations in positions similar to what Einstein did for velocities. To this end, on the same footing of the speed of light c, an upper bound for positions can be introduced. We denote this bound on position by d. Such a construction induces a natural coordinate, the EM coordinates, that will be denoted by x^μ. This system of coordinates uses the same hypersurfaces of constant time as the Milne coordinates, while implementing the scale d in the formulation. In what follows, the reader may realize that the steps are similar to the steps from Galilean mechanics to special relativity and employment of boosts in translation of velocities, but this time for the positions.

3.1. Spherical version

The spherical version of EM coordinates, $x^\mu_{\rm s} = (ct,\ r,\ \theta,\ \varphi)$, is related to the spherical Cartesian coordinates $X^\mu_{\rm s}$ in equation (3) by

$$cT = e^{\frac{ct}{d}} \frac{d}{\sqrt{1 - \frac{r^2}{d^2}}}, \qquad R = e^{\frac{ct}{d}} \frac{r}{\sqrt{1 - \frac{r^2}{d^2}}}, \qquad \theta = \theta, \qquad \varphi = \varphi, \tag{17}$$

in which $0 \leqslant r < d$. The constant d is the upper bound for positions that was advertised before and plays an important role in the analysis of this paper. In spherical EM coordinates, the Minkowski metric is

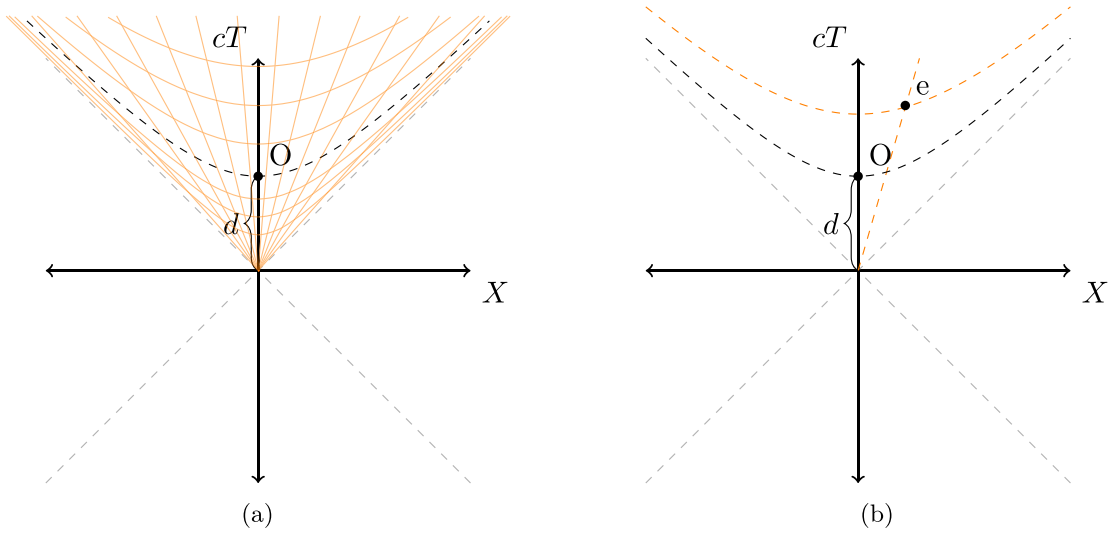

Figure 4. (a) The observer O is assumed to be at the origin ($t=0, x=0$) in Einstein-Milne coordinates. The dashed black line depicts the hypersurface of simultaneity for the observer O. The orange lines show the hypersurfaces of constant t and lines of constant x. (b) An event e is a point that is identified by its associated Einstein-Milne coordinates (ct, x).

$$\mathrm{d}s^2 = \frac{e^{\frac{2ct}{d}}}{f}\left(-fc^2\mathrm{d}t^2 + \frac{\mathrm{d}r^2}{f} + r^2(\mathrm{d}\theta^2 + \sin^2\theta\mathrm{d}\varphi^2)\right), \qquad f = 1 - \frac{r^2}{d^2}. \tag{18}$$

Notice that the term in parenthesis is the four-dimensional de Sitter spacetime in the static coordinates. So, the EM coordinates are the ones in which the Minkowski spacetime is manifestly conformal to the de Sitter spacetime. This is an interesting feature concerning the causal structure of the two cosmological models. Moreover, the EM coordinates cover the patch inside the light cone with its tip at the origin $T=R=0$ (see figure 4).

The trace of the extrinsic curvature of the surfaces of constant t is found to be

$$K = K^{\alpha}_{\ \alpha} = \frac{-3e^{-\frac{ct}{d}}}{d}. \tag{19}$$

The Ricci scalar of these hypersurfaces can also be found to be equal to $\frac{-6e^{-\frac{2ct}{d}}}{d^2}$. So, the spatial curvatures are constant and negative at any given time t, which means that they are the Milne's hyperboloids.

3.2. Cartesian version

A convenient coordinate to study boosts in special relativity is the Cartesian coordinate. For the same reason, in this section we focus on the Cartesian version of the EM coordinates $x^{\mu} = (ct, x, y, z)$ with the notation $\overrightarrow{x} = (x, y, z)$, that is defined by

$$X^{\mu} \equiv \begin{pmatrix} cT \\ X \\ Y \\ Z \end{pmatrix} = e^{\frac{ct}{d}} \frac{1}{\sqrt{1-\frac{r^2}{d^2}}} \begin{pmatrix} d \\ x \\ y \\ z \end{pmatrix}, \tag{20}$$

in which

$$-\infty < t < \infty, \qquad -d < \{x, y, z\} < d \qquad r^2 = x^2 + y^2 + z^2, \qquad 0 \leqslant r < d. \tag{21}$$

The Minkowski metric in this coordinate is

$$\mathrm{d}s^2 = \frac{e^{\frac{2ct}{d}}}{f}\left[-fc^2\mathrm{d}t^2 + \mathrm{d}x^2 + \mathrm{d}y^2 + \mathrm{d}z^2 + \frac{(x\mathrm{d}x + y\mathrm{d}y + z\mathrm{d}z)^2}{d^2 f}\right]. \tag{22}$$

The hypersurfaces of constant time t are the future sector of the hyperboloids that are determined by the constraint

$$X_{\alpha}X^{\alpha} = -d^2 e^{\frac{2ct}{d}}, \tag{23}$$

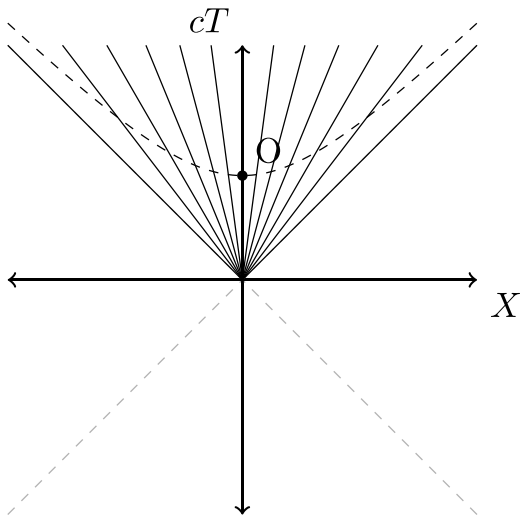

Figure 5. An Einstein-Milne frame can be visualized by the straight worldlines of the observers that pass from the origin.

and hence,

$$t = \frac{d}{2c}\ln\left(\frac{-X_\alpha X^\alpha}{d^2}\right). \tag{24}$$

The lines of constant position are straight, timelike worldlines that pass from the tip of the light cone. An illustration of these surfaces is presented in figure 4.

An interesting feature of the EM coordinates is that the observer at $x^\mu = (0, 0, 0, 0)$ is situated at $X^\mu = (d, 0, 0, 0)$, i.e.

$$X^\mu_{\rm O} = \begin{pmatrix} d \\ 0 \\ 0 \\ 0 \end{pmatrix}. \tag{25}$$

This feature resembles the non-vanishing velocity 4-vector $V^\mu = (c, 0, 0, 0)$ for a particle at rest in an inertial frame of special relativity.

Another feature of the EM coordinate is that it covers only the inside and future of the light cone with the tip at $X^\mu = (0, 0, 0, 0)$. This condition, which is

$$X_\alpha X^\alpha < 0, \qquad \text{and} \qquad 0 < X^0, \tag{26}$$

is the positional analogue of the similar condition on velocities in special relativity: that the velocity of the physical observers is constrained to be less than c and future directed, and hence, $V_{{\rm O}'\alpha}V^\alpha_{{\rm O}'} < 0$ and $0 < V^0_{{\rm O}'}$. However, we realize that the velocity in special relativity is constrained to be on the hyperboloid $V_{{\rm O}'\alpha}V^\alpha_{{\rm O}'} = -c^2$ while the position is not. In a section devoted to the velocity, we will show that the latter constraint on the velocities is relaxed in the EM formulation, which makes the position and velocity more similar.

3.3. Einstein-Milne frames

Similar to the inertial frames in Cartesian coordinate system, it is useful to define a new set of frames that are induced by the EM coordinates. All observers that have constant EM positions, i.e., they are labeled by the coordinates $x^\mu = (ct, x_0, y_0, z_0)$ with constants $\{x_0, y_0, z_0\}$ constitute a frame. We can call it an EM frame and visualize it as all straight timelike worldlines that pass from the origin $X^\mu = (0, 0, 0, 0)$. A schematic of such a frame is depicted in figure 5.

Notice that all of the observers that we consider in this paper, either in an inertial frame or in an EM frame, are inertial observers. However, we did not touch the name of the frames in special relativity and still called them inertial frames. So, one should be careful that the terminology does not mean that the observers in an EM frame are not inertial.

Each EM frame highlights a light cone, that is found by the outermost worldlines in the EM coordinates, i.e., in the limit of positions to d. It is basically the congruence of the light rays that have emitted from some point $(\hat{X},\ \hat{Y},\ \hat{Z})$ and at some time $\hat{T}$. In such a case, the tip of the light cone would be at $\hat{X}^\mu = (c\hat{T},\ \hat{X},\ \hat{Y},\ \hat{Z})$. So, any

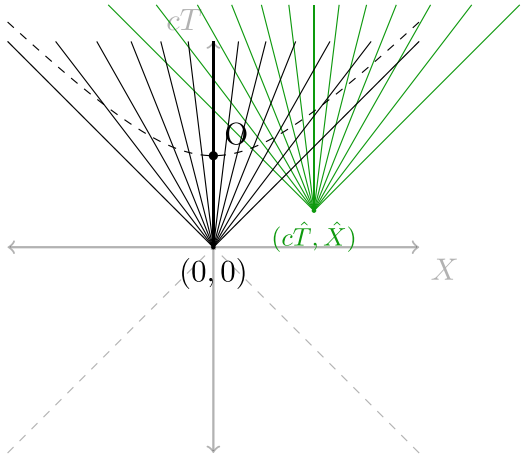

Figure 6. Einstein-Milne frames: In this figure, two frames are depicted, one in black and the other in green. Their tips are situated at $(0, 0)$ and $(c\hat{T}, \hat{X})$, respectively. Any EM frame can be labeled by the coordinate of its tip.

EM frame can be labeled by the coordinate $\hat{X}^\mu$ of its tip. For visualization, two such frames are depicted in figure 6.

A similar question as in the case of the inertial frames arises here, which is about the coordinate of the observer. In contrast with the observers in the inertial frames at the origin, EM observers are considered to be not at the tip $\hat{X}^\mu$, but at the coordinate $\hat{X}^\mu + (d,\ 0,\ 0,\ 0)$. Let us emphasize it as the '*fundamental feature*' of the EM frames here.

Each EM frame in its associated (Cartesian) coordinates has the tip of its light cone at the origin (0, 0, 0, 0) and its observer is at (d, *0, 0, 0)*.

As a result of this feature, the transformations between the EM observers can be different from the Poincaré transformations in (14) that are suited to transform within and between the inertial frames. In the next section, the appropriate EM transformations are investigated.

4. Einstein-Milne transformations

To find the appropriate transformations in the EM formulation, we divide the analysis into two parts: transformations between the observers (i) within an EM frame and (ii) in different EM frames. We notice that the observers in an EM frame are not at rest with respect to each other. This can be easily seen from the different slopes of the worldlines in figure 5. Therefore, the transformations should be such that, in addition to position and time, they should change the velocities in an appropriate way that is related to the change of positions. For clarity, we introduce the spacetime action of the transformations in this section and postpone their action on the velocities to the next section.

4.1. Transformation within a frame

Let us consider an observer O at $x^\mu_{\rm O} = (0,\ 0,\ 0,\ 0)$, that is, at $X^\mu = (d, 0, 0, 0)$ in an EM frame with its tip at $X^\mu = (0, 0, 0, 0)$. An appropriate translation in position and time to another observer $\rm O'$ at the point $x^\mu_{\rm O'} = (ct_{\rm O'},\ x_{\rm O'},\ y_{\rm O'},\ z_{\rm O'})$ that respects the fundamental feature of the EM frame can be given by a scaling and boost-like transformation

$$X'^\mu = e^{\frac{-ct_{\rm O'}}{d}} \Lambda^\mu_\nu(\overrightarrow{x}_{\rm O'}) X^\nu, \tag{27}$$

in which $\Lambda^\mu_\nu(\overrightarrow{x}_{\rm O'})$ is the boost in the direction of $\overrightarrow{x}_{\rm O'}$ with the magnitude

$$\gamma = \frac{1}{\sqrt{1-\beta^2}}, \qquad \beta = \frac{r_{\rm O'}}{d}. \tag{28}$$

The scaling acts as a translation in time, and the boost changes the position of the observer. Of course, Λ^μ_ν represents the Lorentz group that includes rotations too. However, in this paper our focus is on the boosts and ignore the rotations that can always be considered trivially.

As an example, let us consider the observer $\rm O'$ at $x^\mu_{\rm O'} = (ct_{\rm O'},\ x_{\rm O'},\ 0,\ 0)$. In this case, the boosts are explicitly

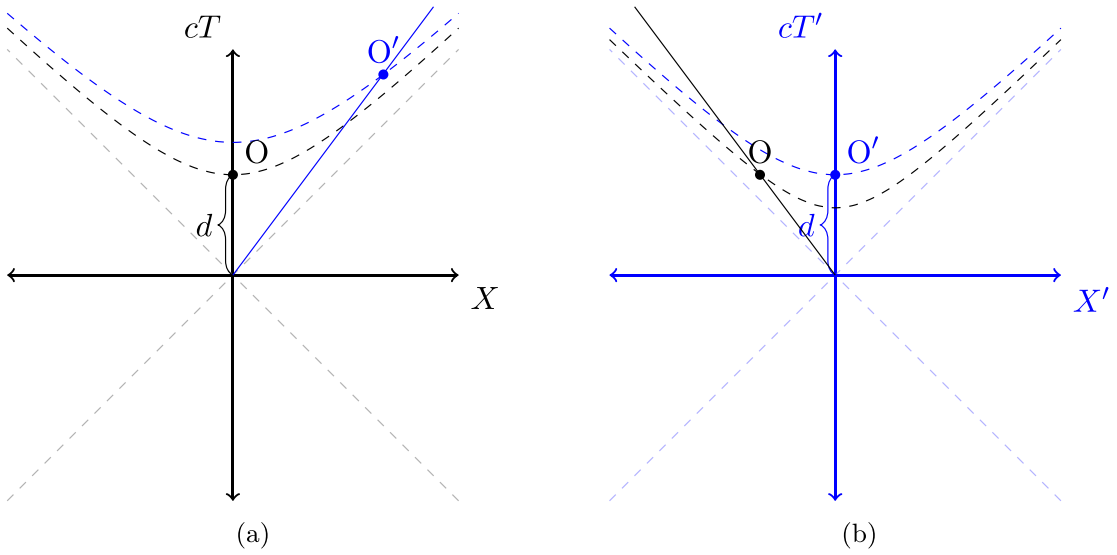

Figure 7. Translations from an observer O to O′ in EM coordinates, in contrast with figure 2. (a) From the point of view of O, the observer O′ is situated at $(ct_{O'}, x_{O'})$ with the worldline depicted by a solid blue line. (b) After the translations, the observer O′ is at the origin of his EM coordinate, i.e., at $t' = 0$ and $x' = 0$, while the observer O is at $(-ct_{O'}, -x_{O'})$ in primed coordinates and follows the solid black worldline.

$$\Lambda^{\mu}_{\nu}(x_{O'}) = \begin{pmatrix} \gamma & -\gamma\beta & 0 & 0 \\ -\gamma\beta & \gamma & 0 & 0 \\ 0 & 0 & 1 & 0 \\ 0 & 0 & 0 & 1 \end{pmatrix}, \qquad \gamma = \frac{1}{\sqrt{1-\beta^2}}, \qquad \beta = \frac{x_{O'}}{d}, \tag{29}$$

and we find

$$cT' = \gamma e^{\frac{-ct_{O'}}{d}}(cT - \beta X), \qquad X' = \gamma e^{\frac{-ct_{O'}}{d}}(X - \beta cT), \qquad Y' = e^{\frac{-ct_{O'}}{d}}Y, \qquad Z' = e^{\frac{-ct_{O'}}{d}}Z. \tag{30}$$

As a result of the transformation above, an event at $x^{\mu} = (ct, x, y, z)$ is mapped to $x'^{\mu} = (ct', x', y', z')$ by

$$t' = t - t_{O'}, \qquad x' = \frac{x - x_{O'}}{1 - \frac{x\beta}{d}}, \qquad y' = \frac{y}{\gamma(1 - \frac{x\beta}{d})}, \qquad z' = \frac{z}{\gamma(1 - \frac{x\beta}{d})}. \tag{31}$$

It is easy to check that in the new coordinates, the observer O′ is situated at $X'^{\mu'}_{O'} = (d, 0, 0, 0)$ and the tip of the frame light cone is at the origin $\hat{X}'^{\mu} = (0, 0, 0, 0)$. In other words, the transformation (27) respects the EM fundamental feature that was emphasized in the previous section. A schematic of such an EM 'space and time translation' from O to O′ is depicted in figure 7.

4.2. Transformation of the metric

The boost sector of the coordinate transformations in equation (27) from X^{μ} to X'^{μ} keeps the Cartesian metric diag$(-1, 1, 1, 1)$ intact. But, the scaling sector multiplies it by a factor $e^{\frac{2ct_{O'}}{d}}$. To undo the change of scales between observers at different hyperboloids, in addition to the diffeomorphism (27) a rigid Weyl scaling with a factor $e^{-\frac{2ct_{O'}}{d}}$ is necessary, that is

$$g_{\mu\nu} \to e^{-\frac{2ct_{O'}}{d}} g_{\mu\nu}. \tag{32}$$

Such a scaling removes the $t_{O'}$ from the resulted metric that is written in coordinates $x'^{\mu} = (ct', x', y', z')$, and yields a metric that is exactly the same as (22) with the replacement $(ct, x, y, z) \to (ct', x', y', z')$. From the physical point of view, such a scaling is necessary to prevent any value of t from being privileged and makes all observers at different time slices to be physically equivalent.

4.3. Velocity

In the EM model, the velocity 4-vector has a delicate difference in its components when compared to the special relativity. Let us consider a massive point particle in motion with the velocity

$$\begin{cases} u_X = \frac{\mathrm{d}X}{\mathrm{d}T} \\ u_Y = \frac{\mathrm{d}Y}{\mathrm{d}T}, \\ u_Z = \frac{\mathrm{d}Z}{\mathrm{d}T} \end{cases} \qquad \overrightarrow{u} \equiv (u_X, u_Y, u_Z), \qquad u \equiv \sqrt{u_X^2 + u_Y^2 + u_Z^2}. \tag{33}$$

Assume also that the particle is at some point $x_0^\mu = (ct_0, x_0, y_0, z_0)$ from the point of view of the observer O, that she herself is at $x^\mu = (0, 0, 0, 0)$. The velocity 4-vector of such a particle is defined as

$$U^\mu \equiv \frac{\mathrm{d}X^\mu}{\mathrm{d}\sigma} = \frac{e^{\frac{ct_0}{d}}\mathrm{d}X^\mu}{\mathrm{d}\sigma_{\mathrm{O}}} = \frac{e^{\frac{ct_0}{d}}}{\sqrt{1 - \frac{u^2}{c^2}}}\begin{pmatrix} c \\ u_X \\ u_Y \\ u_Z \end{pmatrix}, \tag{34}$$

in which σ is the proper time of a moving object on its hyperboloid of constant time, and,

$$\mathrm{d}\sigma_{\mathrm{O}}^2 = -\mathrm{d}X^\mu \mathrm{d}X_\mu. \tag{35}$$

We note that by the scaling equation (32) the proper time is different for the observers at different time t. As a result of this scaling, the proper time of the motion of the aforementioned particle from the point of view of the observer O, denoted by $\mathrm{d}\sigma_{\mathrm{O}}$, is given by

$$\mathrm{d}\sigma_{\mathrm{O}} = e^{\frac{ct_0}{d}}\mathrm{d}\sigma, \tag{36}$$

which provides the second equality in equation (34). So, although the definition of the velocity is similar to the special relativity, there is an extra $e^{\frac{ct_0}{d}}$ when written in from the point of view of the observer O. The last equation in equation (34) is the replacement of σ_{O} by $\mathrm{d}T$ via the relation

$$\mathrm{d}\sigma_{\mathrm{O}} = c \sqrt{1 - \frac{u^2}{c^2}} \mathrm{d}T, \tag{37}$$

that is a rearrangement of equation (35). The necessity of the presence of the factor $e^{\frac{ct_0}{d}}$ in 4-velocities can be realized by the expectation that an observer that is attached to the moving object should attribute the 4-velocity $(c, 0, 0, 0)$ to it, and so, such a factor is needed to cancel the scaling $e^{-\frac{ct_0}{d}}$ in the transformation equation (27) to such an observer. An interesting feature of this modification is that the U^μ is no longer constrained to satisfy $U_\alpha U^\alpha = -c^2$. Instead, we find

$$U_\alpha U^\alpha = -c^2 e^{\frac{2ct_0}{d}}. \tag{38}$$

4.4. General transformations

The group of transformations in equation (27) acts within an EM frame and is composed of the Lorentz group and the scaling. The rotation subgroup of the Lorentz group acts as the usual rotation, while the boost part does the job of translations in EM position. Besides, the scaling serves as the translation in EM time.

The next step is to generalize the transformations that include changing from an EM frame to another one. In other words, we would like to ask about how to transfer to an observer that his worldline does not necessarily pass from the tip of the initial frame. To answer this question, let us consider the initial EM frame with the tip of its light cone at the origin $X^\mu = (0, 0, 0, 0)$ and its observer O at $X^\mu = (d, 0, 0, 0)$. Another observer O' is at some point $X^\mu_{\mathrm{O}'}$, or by the relation (20) at some $x^\mu_{\mathrm{O}'}$, inside the future light cone of the initial frame, i.e., his coordinate respects the condition (26). His velocity 3- and 4-vectors are denoted by $\overrightarrow{v} = (v_X, v_Y, v_Z)$ and $V^\mu_{\mathrm{O}'}$ respectively. The configuration of the two observers is illustrated in figure 8.

Given the setup that is described above, the transformation from the observer O to O' is given by

$$X'^\mu = e^{-\frac{ct_{\mathrm{O}'}}{d}}\Lambda^\mu_\nu(\overrightarrow{v})(X^\nu - \hat{X}^\nu), \tag{39}$$

in which

$$\hat{X}^\nu = X^\nu_{\mathrm{O}'} - \frac{d}{c}V^\nu_{\mathrm{O}'} \tag{40}$$

is the coordinate of the tip of the new frame to which O' belongs. The intuition of the generic transformation (39) is as follows: The EM frame that the O' could be one of its observers is not unique. However, the $\hat{X}^\nu$ is the tip of the frame to which O' belongs, and in addition, he is on a hyperboloid with a similar curvature as his original one in the initial frame (see figure 9). By equation (19) it means to be at the similar time $t_{\mathrm{O}'}$. This can be examined by calculating the square of the norm of $X^\mu_{\mathrm{O}'} - \hat{X}^\nu$ via equation (23) and finding that the result is the same as for the $X^\mu_{\mathrm{O}'}$ itself. Having the tip of the new frame in hand, the $X^\nu - \hat{X}^\nu$ in (39) is a shift to this new frame. Then, within this frame, the O' is transferred to the coordinate $X'^\mu = (d, 0, 0, 0)$. The $\Lambda^\mu_\nu(\overrightarrow{v})$ and the time scaling do this latter job. A schematic of the initial and new EM frames is depicted in figure 9.

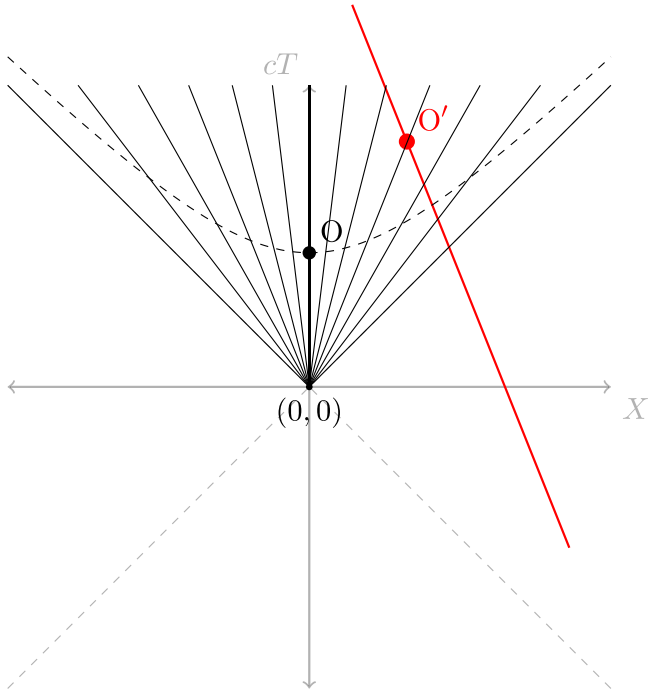

Figure 8. A generic EM transformation changes from the observer O to an arbitrary observer O′ that is inside the future part of the light cone of the initial frame. The worldline of O′ does not pass from the tip of the light cone at the origin, and so it belongs to another EM frame.

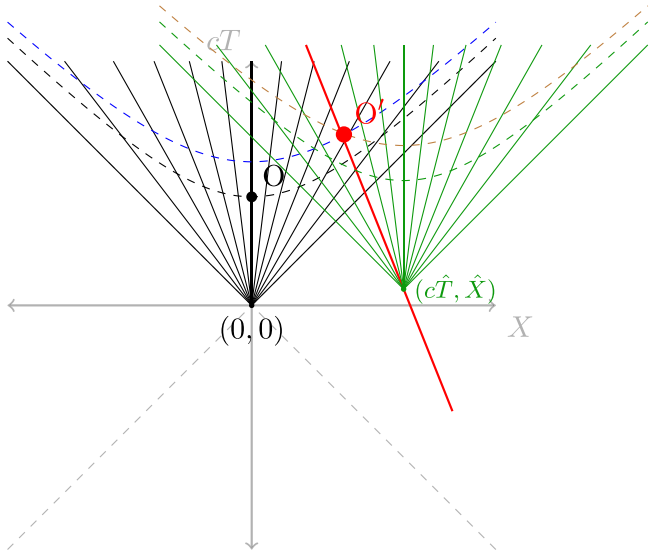

Figure 9. The observer O′, which he and his worldline are colored in red, belongs to a frame that is depicted by green color. The frame is introduced such that he is at a hyperboloid, the brown, that is similar to his original hyperboloid, the blue. If the tip of this frame happens to be at the origin, the generic EM transformations reduce to the translations within an EM frame.

In the next section, we will clarify why $\overrightarrow{v}$ and $\overrightarrow{x}$ can be used interchangeably within a frame. However, at the end of this section, let us have a closer look at the generic EM transformations in (39).

- In the special case $\hat{X}^{\mu} = (0,\ 0,\ 0,\ 0)$, the equation (39) reproduces the transformations within an EM frame in equation (27). It is easy to visualize how the two frames in figure 9 coincide when $\hat{X}^{\mu} = (0,\ 0,\ 0,\ 0)$.
- The generic EM transformations in (39) have the group structure of Poincaré. Note that the parameter $t_{\mathrm{O}'}$ in the scaling is not independent from the Poincaré input parameters $\overrightarrow{v}$ and $X^{\mu}_{\mathrm{O}'}$.

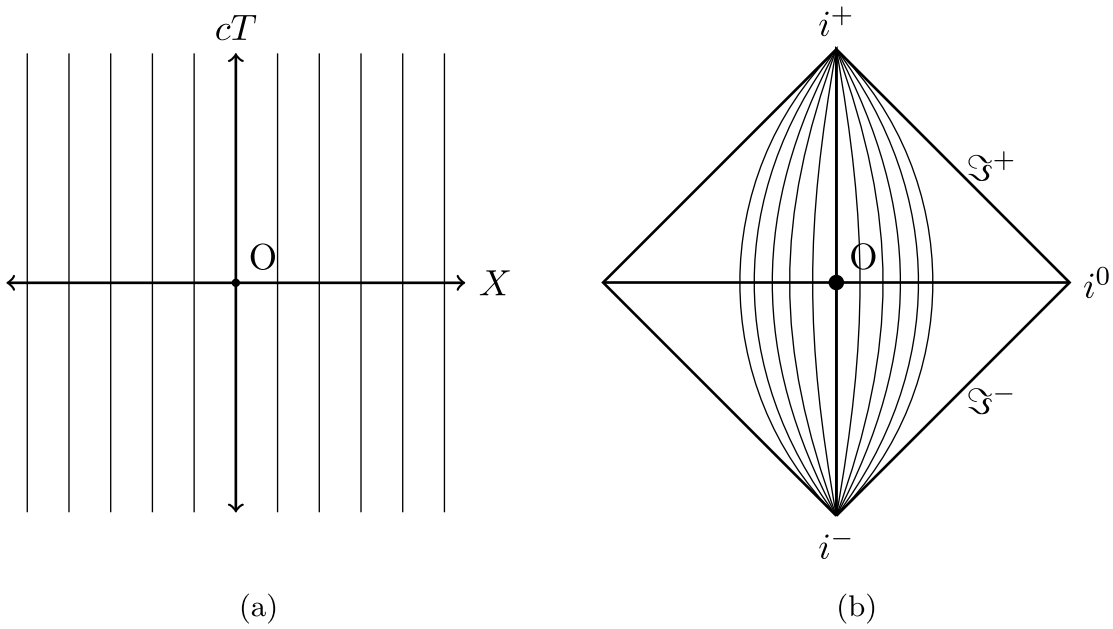

Figure 10. (a) The 2-dimensional Minkowski in Cartesian coordinates: the vertical solid lines show the worldlines of some uniformly distributed matter. (b) The same physical setup in the Carter-Penrose diagram: the diagram induces an illusion of the explosion of the Universe from the point i^-.

- Although the transformation (39) resembles the transformation in (15) in group structure, they are different in the context of the inertial frames and EM frames.

  Inertial frames: The standard (shift-like) translations (15) act within an inertial frame, while boosts (16) change one frame to another.

  EM frames: The standard (shift-like) transformations change the frame, while the boosts (27) (and scaling) act within a frame.

The rotation part of the Lorentz group acts in the same way in both of the frame types. The words above give some intuition of the difference between the two types of frames, while the reader notices that all of the transformations can be considered a change of frame depending on the definition of a frame. For example, if a rotated coordinate is considered a new frame, then it could be said that the rotation changes the frame. But this is not the usual terminology in special relativity, and we have used similar terminology in the description above.

5. No center in the EM universe

In the introduction, a question was posed to the Milne model: Are the observers at $R=0$ privileged because the Universe has exploded at their position long ago? These observers (in contrast with other inertial observers in the same inertial frame) have an isotropic panorama of the recessing galaxies. In EM formulation, the answer to this question is 'no, we are not privileged,' even though it is a problem for the Milne model. The aim of this section is to clarify the difference between the two models that resolves this issue.

To see how the EM model answers this question, let us pose the question in a simpler setup that the reader is probably more familiar with. Consider the 2-dimensional Minkowski spacetime in the Cartesian coordinates (cT, X) filled with some matter that is homogeneously spread along the X axis. The setup is depicted in figure 10. However, this homogenous setup looks different in Carter-Penrose coordinates $(c\mathcal{T}, \mathcal{X})$ via the transformations

$$c\mathcal{T}=\frac{\tan^{-1}\left(\frac{cT+X}{2}\right)+\tan^{-1}\left(\frac{cT-X}{2}\right)}{2},\quad \mathcal{X}=\frac{\tan^{-1}\left(\frac{cT+X}{2}\right)-\tan^{-1}\left(\frac{cT-X}{2}\right)}{2},\ c\mathcal{T},\mathcal{X}\in\left(-\frac{\pi}{2},\frac{\pi}{2}\right), \tag{41}$$

which is illustrated in figure 10.

Looking at the Carter-Penrose diagram without having any additional information from the Cartesian coordinate could, in principle, induce that the observer $O=(0,0)$ is at the center of the Universe because all of the matter of the Universe has (apparently) originated from the same spatial point $\mathcal{X}=0$, that is $i^-=(-\frac{\pi}{2},0)$. Here, the reader is invited to think about a method to reject this false deduction without referring to the

Cartesian coordinates, having in mind that, per se, no coordinate is preferred to any other coordinates in general relativity.

The above fallacy can be rejected using the proposition: *translations in spacetime are governed by the transformations that are generated by ∂_T and ∂_X*. To this end, we may use the proof by contradiction as follows.

- Assumption 1: $i^- = (-\frac{\pi}{2}, 0)$ is at the center of the Universe.
- Corollary 1: Any observer who has Carter-Penrose spatial coordinate $\mathcal{X}$ equal to the i^- is at the center of the Universe.
- Corollary 2: The observer O in figure 10 is at the center of the Universe.
- Corollary 3: Another observer O′ at $\mathcal{X} \neq 0$ is not at the center of the Universe.
- Assumption 2: Translations in spacetime are governed by the transformations that are generated by ∂_T and ∂_X.
- Corollary 4: The point i^- is invariant under the spacetime translations in Assumption 2.
- Corollary 5: The observer O′ can always be translated to the similar Carter-Penrose spatial coordinate as i^-, that is $\mathcal{X} = 0$.
- Corollary 6: By corollaries 1, 4, and 5, the observer O′ is at the center of the Universe.

But corollary 6 is in contradiction with corollary 3, showing that one of the assumptions (here, Assumption 1) is false. The lesson that we learn from the above analysis is that apparent divergence (or convergence) of matter from (or into) a point in an illustrative diagram may be an illusion and artifact of the choice of coordinates.

After this warming-up example, we can look again at figure 5. It resembles figure 10 in the sense that there is a point $X^\mu = (0, 0)$ from which (apparently) the matter of the Universe is originating. However, in this case (and based on the proposal of this paper), the Cartesian coordinates X^μ are the illusive ones, and the EM coordinates x^μ are those that are assumed to govern the translations. The same proof can be used to show that neither the point $X^\mu = (0, 0)$ nor the observer O at some point $X^\mu = (cT, 0)$ reside at a point that can be considered as the center of the Universe. For completeness, the steps are explained below.

- Assumption 1: $X^\mu = (0, 0)$ is the center of the Universe.
- corollary 1: Any observer who has a Cartesian spatial coordinate X (or in 4-dimensional case, the radius R) equal to zero is at the center of the Universe.
- corollary 2: The observer O in figure 5 is at the center of the Universe.
- corollary 3: Another observer O′ at $X \neq 0$ is not at the center of the Universe.
- Assumption 2: Translations in spacetime are governed by the transformations that are generated by EM translations, that are the boosts in (30).
- corollary 4: The point $X^\mu = (0, 0)$ is invariant under the spacetime translations in Assumption 2.
- corollary 5: The observer O′ can always be translated to the Cartesian spatial coordinate $X' = 0$.
- corollary 6: The corollaries 1, 4, and 5, the observer O′ is at the center of the Universe,

which is in contradiction with corollary 3. So, one of the assumptions (that is proposed to be Assumption 1 in this paper) is incorrect. It is important to emphasize the role of Assumption 2 in the above argument, that distinguishes the EM coordinate. Besides, this assumption is the main difference between the EM and the Milne model and resolves the 'center of universe' problem that was alluded to in the introduction.

So far we showed that the illusive central point of the divergence of matter in figure 5 does not result in the existence of a center for the Universe. Nonetheless, it distinguishes one of the EM frames from the other ones; the one whose tip is identified by $X^\mu = (0, 0)$. Does it make this EM frame a privileged one? To answer this question, we recall that in the standard cosmology, there is one privileged inertial *frame* that its observers detect the recession redshift isotropic, and other inertial frames that have non-vanishing velocity w.r.t. it would miss this nice isotropic picture. In other words, in the standard cosmology, there is a privileged frame, while all observers within that frame are equivalent. Therefore, the existence of a privileged frame in the Universe is not considered so discriminating. The same is true in the EM model. It is an EM frame that is privileged by the observation: the one with its tip at the point of explosion. However, it does not mean that we, as some observers

in this frame, are fortunate in our position in the Universe. In other words, all distant observers in our EM frame are as lucky as us and enjoy an isotropic view of redshifted galaxies.

5.1. Hubble's law without ultra relativistic speeds

The velocity 4-vector in equation (34) is a covariant vector that transforms similar to the X^μ in equation (27)

$$U'^\mu = e^{\frac{-ct_{O'}}{d}}\Lambda^\mu_\nu(\overrightarrow{x}_{O'})U^\nu, \tag{42}$$

This can also be derived by noting that in the definition of U^μ in equation (34) $d\sigma$, that is defined on the similar hyperboloid of the particle, is invariant and does not change, while dX^μ changes similar to the X^μ.

To find how $\overrightarrow{u}$ is transformed, we note that $e^{\frac{-ct_{O'}}{d}}$ in (42) is combined with the scaling factor in (34) to constitute the new time $t'_0 = t_0 - t_{O'}$ of the particle. So, it suffices to focus on the $\Lambda^\mu{}_\nu(\overrightarrow{x}_{O'})$ part of the transformations in equation (27) on velocities. This transformation is just the action of a boost with the parameter $\beta = \frac{r_{O'}}{d}$ in the $\overrightarrow{x}_{O'}$ direction. Explicitly, for the simple case of the translation in x direction as in equation (29), it is

$$u'_X = \frac{u_X - \frac{c}{d}x_{O'}}{1 - \frac{u_X x_{O'}}{cd}}, \qquad u'_Y = \frac{u_Y}{\gamma(1 - \frac{u_X x_{O'}}{cd})}, \qquad u'_Z = \frac{u_Z}{\gamma(1 - \frac{u_X x_{O'}}{cd})}. \tag{43}$$

However, this is exactly the action of boosts by the speed v_X that is related to $x_{O'}$ by $v_X = \frac{c}{d}x_{O'}$. This is an important result of the analysis in this paper; in EM formulation, a translation in position induces a translation in velocity that are related to each other by a factor $\frac{c}{d}$. In other words, transformation from an observer O to another observer O′ at $x = x_{O'}$ with $\beta = \frac{x_{O'}}{d}$ changes the inertial frame to another one with the velocity $v = \beta c$. Therefore, the EM translations (27) are translations in both of the positions and velocities. For an EM translation towards an arbitrary direction, this relation can be isotropically written as

$$v = \frac{c}{d}r. \tag{44}$$

This result is the celebrated Hubble's law $v = H_0 r$ in EM relativity with

$$H_0 = \frac{c}{d}. \tag{45}$$

Notice that in contrast with the standard Hubble's law in open universes, the speed v in equation (44) cannot exceed the light speed c because the positions (here, $x_{O'}$ or r) are bounded above by d in equation (21).

Hubble's relation in standard cosmology indicates superluminal speeds w.r.t an observer. But it is not a problem in standard cosmology because of the expansion of the geometry (see, e.g., [75, 91]). In the next section, we study the dynamics of the EM model in GR and show that the values of d and the current density of matter are such that the geometry at the current time can be well approximated to be a Minkowski. So, the forbidden superlumnial Hubble's velocity, which is a characteristic of the EM (and also the Milne) model, turns out to be useful in explanation of the observed cosmological redshift.

6. Dynamics in general relativity

The Minkowski geometry, independent of its coordination, is a vacuum solution to GR. However, it is no longer a solution if there is some matter in the Universe, as we see manifestly there is. The presence of matter brings about dynamics in such a static geometry. General relativity, which is the most successful theory of gravity, is one of the many gravitational theories that are built to model the dynamics of the matter and geometry of the Universe. It is explained by the Einstein-Hilbert action and Lagrangian

$$I = \int d^4x\sqrt{-g}\,\mathcal{L}, \qquad \mathcal{L} = \frac{c^4}{16\pi G}R + \mathcal{L}_M, \tag{46}$$

where R is the Ricci scalar (not to be confused by R as a radial coordinate), G is the Newton constant, and $\mathcal{L}_M$ is the Lagrangian of the matter. The field equation of this theory is the celebrated Einstein equation

$$G_{\mu\nu} = \frac{8\pi G}{c^4}T_{\mu\nu}, \tag{47}$$

in which $G_{\mu\nu}$ and $T_{\mu\nu}$ are Einstein tensor and energy-momentum tensor of the matter fields, respectively. Assuming the cosmological principle in the EM model, we consider the matter field to be a homogeneous and isotropic perfect fluid,

$$T^\mu_{\ \nu} = \text{diag}(-\rho c^2, P, P, P). \tag{48}$$

On the same footsteps of the standard model of cosmology, we assume that the dynamics respects the isotropy and homogeneity of the surfaces of constant t in the EM metric (18). Therefore, the EM metric can only be modified by a factor $a(t)$ that scales the maximally symmetric hyperboloids of constant time. So, the ansatz of the dynamical EM metric is

$$\mathrm{d}s^2 = \frac{e^{\frac{2ct}{d}}}{f}\left(-fc^2\mathrm{d}t^2 + a^2(t)\left[\frac{\mathrm{d}r^2}{f} + r^2(\mathrm{d}\theta^2 + \sin^2\theta\mathrm{d}\varphi^2)\right]\right), \qquad f = 1 - \frac{r^2}{d^2}. \tag{49}$$

By inserting this ansatz in the Einstein equation (47), the analogue of the first Friedmann equation in equation (10) is found from the 00 component of the equations as

$$\left(\frac{\dot{a}}{a} + \frac{c}{d}\right)^2 + \frac{kc^2}{d^2a^2} = \frac{8\pi G}{3}\rho \quad e^{\frac{2ct}{d}} \tag{50}$$

for $k = -1$.

The r.h.s of (50) is negligible w.r.t other terms by the observation of baryons and radiation, that are the visible (i.e., not including the dark) matter and energy in the Universe. To see this, by equation (45) the $(kc^2)/(d^2a^2)$ term can be written as $(kH_0^2)/(a^2)$ in which k is equal to -1, and $a(t)$ at present is chosen to be equal to 1. Besides, t in r.h.s of (50) is set to 0 at present. So, comparison of the aforementioned term with the r.h.s of (50) is the comparison of $(3H_0^2)/(8\pi G)$ and ρ. In the standard model of cosmology, the former is called the critical density ρ_c. Observational data shows that the energy density of the visible matter and radiation in the Universe is about 5 percent of the ρ_c. Therefore, the field equation (50) is approximately

$$\left(\frac{\dot{a}}{a} + \frac{c}{d}\right)^2 + \frac{kc^2}{d^2a^2} \approx 0. \tag{51}$$

The generic solution to this equation is

$$a(t) = 1 + a_0 e^{-\frac{ct}{d}}. \tag{52}$$

The constant a_0 is the integration constant that can be absorbed by the diffeomorphism

$$t \to t + \frac{d}{c}\ln(1 + a_0 e^{-\frac{ct}{d}}). \tag{53}$$

Hence, it can be set to zero, and the EM metric (18) is recovered. The solution (52) satisfies other components of the field equation (47) in the dust approximation of the matter, that is, $P \approx 0$. This approximation is a valid approximation, noting that the density of radiation is of order 10^{-2} smaller than the density of baryons in the Universe.

In summary, the visible matter content of the Universe is so dilute at present time that it can be ignored at first order in the EM model. In this regard, it is possible to apply the formulation explained in the previous sections to study kinematics at large scales. While the Universe's matter and radiation content influence spacetime dynamics, we'll focus solely on kinematics in this paper, reserving dynamic investigations for future work. In the next section, we explore one of the most interesting implications of the model, which is the cosmological redshift.

7. Cosmological redshift: theory and observation

7.1. Translational redshift as a Doppler effect

In section 5.1 it was shown that an EM translation in space is concomitant with a change of velocity that is related via Hubble's law in equation (44). So, in the EM model, the boosts have a double job: translations in space and velocity. However, the boosts also change the frequency of a beam of light by their action on its 4-momentum vector. This effect is known as the relativistic Doppler effect.

Interestingly, in EM formulation, the frequency of a *perceived* light is always redshifted (i.e., not blueshifted), if the source is at a distance in the same EM frame. To investigate this, imagine a spherical source of light of frequency ν, e.g., a galaxy, and an observer O in its vicinity. Consider also another observer O′ in the same EM frame that is coordinated by a position r (as defined in equation (21)) in a cosmological distance from the Galaxy. Assuming the isotropy, let us consider the observer O′ to reside in the positive X direction, and so, $r = x_{\mathrm{O}'}$. In the vicinity of the source, the angular frequency and the wave number of the light beam are given by the standard relations $\omega = 2\pi\nu$ and $k = \frac{2\pi}{\lambda}$ respectively, where the wavelength λ is given by $\lambda = \frac{c}{\nu}$. Therefore, around the source, the momentum 4-vector k^μ of the light propagating towards the O′ is given by $k^\mu = (\hbar\omega, \hbar kc, 0, 0)$. Such a 4-vector transforms covariantly as

$$k'^{\mu} = e^{\frac{-ct_{O'}}{d}} \Lambda^{\mu}_{\nu}(r) k^{\nu}. \tag{54}$$

However, similar to the velocity in (34), k^{ν} and k'^{ν} have an extra scaling in their definition whenever they are not on the same hyperboloid as the observer. In this regard, the scaling in the transformation (27) only shifts the EM time t in that factor and does not affect the frequencies. So, the frequency that the observer O' perceives is different from the one emitted from source by the action of the translation $\Lambda^{\mu}_{\nu}(r)$. By replacing $\Lambda^{\mu}_{\nu}(r)$ from (29) and using the definitions $\omega' = 2\pi\nu'$ and $k' = \frac{2\pi}{\lambda'}$ and the relation $\lambda' = \frac{c}{\nu'}$ in $k'^{\mu} = (\hbar\omega',\ \hbar k' c,\ 0,\ 0)$, we find the translational redshift formula in the EM model to be

$$\nu' = \sqrt{\frac{1 - \frac{r}{d}}{1 + \frac{r}{d}}}\,\nu. \tag{55}$$

The radius r is a positive number. So, this Doppler effect yields $\nu' < \nu$, i.e., a redshift in the *detected* light.

Let us clarify why the words 'perceived' and 'detected' are emphasized above. The light rays that propagate in the opposite direction of the residence point of an observer are blueshifted. To see this, such a ray in our setup that was described above propagates in the negative X direction and has a momentum $k^{\mu} = (\hbar\omega, -\hbar kc, 0, 0)$. It is easy to check that the frequency is blueshifted by the boost of the translation (54) simply by exchanging the plus and minus signs in (55). However, such a beam will never be perceived by O' unless there could be a mirror effect somewhere that could be considered as a new source of the beam, and again brings the redshift to the calculation, and the overall shift will be towards red.

7.2. Luminosity distance in EM model

One way to find the distances from shining point-like objects is to measure their light intensity while knowing their intrinsic luminosity. Then, based on how fast the light intensity falls in its radial propagation, the distance from the objects can be deduced. However, the radial dependence of the fall-off depends on the formulation and model. Here, the aim is to study this topic in the EM formulation. This analysis elucidates how the model can explain some related observational data in the next section.

Basics: Absolute luminosity L of a point-like isotropic celestial object is defined to be the total energy per second emitted by it. If the flux of energy received from the object is denoted by $\mathcal{F}$, that is the amount of energy per second passing a unit area of the detector, then

$$\mathcal{F} = \frac{L}{4\pi d_L^2}, \tag{56}$$

in which d_L is called the luminosity distance. Besides, using the $\mathcal{F}$ the apparent magnitude m of the object is defined as

$$m = -2.5 \log\left(\frac{\mathcal{F}}{\mathcal{F}_{10\,\mathrm{pc}}}\right), \tag{57}$$

where $\mathcal{F}_{10\,\mathrm{pc}}$ is the flux of energy received from the object if it is situated at a luminosity distance of 10 parsecs (10pc) from the observer. Similarly, the absolute magnitude M is defined by

$$M = -2.5 \log\left(\frac{L}{L_{10\,\mathrm{pc}}}\right), \qquad (L_{10\,\mathrm{pc}} = \mathcal{F}_{10\,\mathrm{pc}} \times 4\pi (10\,\mathrm{pc})^2). \tag{58}$$

Putting the three equations above together, one finds

$$m = M + 5 \log\left(\frac{d_L}{10\,\mathrm{pc}}\right), \tag{59}$$

and if d_L is measured in mega parsecs (Mpc),

$$m = M + 5 \log(d_L) + 25. \tag{60}$$

In addition to the magnitudes, the frequency of the received light can be measured in the detector. The ratio of the emitted and received frequencies is parameterized by the redshift factor z,

$$1 + z = \frac{\lambda'}{\lambda} = \frac{\nu}{\nu'}, \tag{61}$$

which, in the EM model via equation (55), it is

$$1 + z = \sqrt{\frac{1 + \frac{r}{d}}{1 - \frac{r}{d}}}. \tag{62}$$

Luminosity distance: The inverse of equation (62) yields the relation between EM distance r and the redshift factor z as

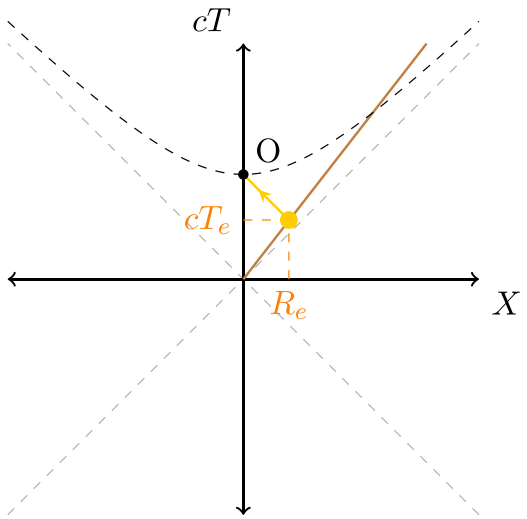

Figure 11. A light ray is emitted from a source at cT_e and R_e and is received by the observer O. The luminosity distance is a distance that the light is attenuated proportional to its square and is different from R_e because of the distance and relative motion of the source.

$$r = \frac{(1+z)^2 - 1}{(1+z)^2 + 1} d. \tag{63}$$

However, the distance that is usually measured in the lab is the luminosity distance d_L. In order to find the $d_L(z)$ instead of $r(z)$, one needs to have $d_L(r)$. In the EM model, the relation between d_L and r is given by

$$d_L = \frac{r}{1 - \frac{r}{d}}, \tag{64}$$

which is derived below. Therefore, by replacing equations (45) and (63) in equation (64), the relation between the luminosity distance d_L and the redshift factor z is found to be

$$d_L = \frac{c}{H_0} \times \frac{z(z+2)}{2} = \frac{z(z+2)d}{2}. \tag{65}$$

Derivation of equation (64): Similar to special relativity, in the EM model there are two reasons that the light from a distant moving source is detected to be attenuated as seen by the receiver: the distance and the relative motion. The former yields the fall-off of intensity when a spherical wave propagates. The latter includes redshift, relativistic beaming (or headlight effect and Doppler boosting), and differences in the measurements of time intervals.

To analyze these phenomena in the EM model, consider the receiver to be the observer O in her point (25) of the EM frame with the coordination X^μ. In addition, imagine a source of light in the same frame but at a constant distance r. According to the relation (44) such a source has a non-vanishing velocity $v = \frac{c}{d} r$ as seen by O. Let us consider a light ray emitted from the source and perceived by the observer O. It is a practice of trigonometry (see figure 11) to find from (20) and (44) that, given the r, the coordinate of the source at the moment of emission X_e^μ (the subscript 'e' for emission) is given by

$$cT_e = \frac{d}{1 + \frac{r}{d}}, \qquad R_e = \frac{r}{1 + \frac{r}{d}}. \tag{66}$$

Using these relations in the equation (23) for X_e^μ and dividing it with the similar equation for the $X_{\rm O}^\mu = (d, 0, 0, 0)$ we find

$$e^{\frac{c(t_e - t_{\rm O})}{d}} = \sqrt{\frac{1 - \frac{r}{d}}{1 + \frac{r}{d}}}. \tag{67}$$

Figure 11 clarifies the setup and how these relations can be calculated by noting that the light rays move on lightlike worldlines.

Now, let us focus on the observer in the vicinity of the source. He finds the energy flow towards the receiver by measuring the amount of energy ΔE_e that passes a solid angle $\mathrm{d}\Omega_e$ and dividing it by the unit of his time Δt_e. The question is how this measured energy flow is seen from the point of view of the O, which her corresponding quantities are denoted by ΔE, $\mathrm{d}\Omega$, and Δt, respectively. To find the answer, we study the transformations of each term separately.

Table 1. Observational data for the redshift factor z and the effective apparent magnitude m_B of the low and high redshift supernovae imported from tables 3, 4, and 5 of the Supernova Cosmology Project paper [94]. (A) Low-z SNe from Hamuy [95] and Riess [96]. (B) New Fits to Perlmutter [2] SNe, (C) The additional 11 SNe by the Hubble space telescope reported in [94].

A		
SN	z	m_B^{eff}
1990O	0.030	16.33 ± 0.20
1990af	0.050	17.39 ± 0.18
1992P	0.026	16.14 ± 0.19
1992ae	0.075	18.35 ± 0.18
1992ag	0.026	16.34 ± 0.20
1992al	0.014	14.42 ± 0.23
1992aq	0.101	19.12 ± 0.17
1992bc	0.020	15.18 ± 0.20
1992bg	0.036	16.66 ± 0.20
1992bh	0.045	17.64 ± 0.18
1992bl	0.043	17.03 ± 0.18
1992bo	0.018	15.42 ± 0.21
1992bp	0.079	18.16 ± 0.18
1992br	0.088	18.93 ± 0.20
1992bs	0.063	18.26 ± 0.18
1993B	0.071	18.40 ± 0.18
1993O	0.052	17.53 ± 0.18
1993ag	0.050	17.73 ± 0.18
1994M	0.024	16.07 ± 0.20
1994S	0.016	14.83 ± 0.22
1995ac	0.049	17.17 ± 0.18
1995bd	0.016	15.37 ± 0.30
1996C	0.030	16.74 ± 0.19
1996ab	0.125	19.47 ± 0.19
1996bl	0.035	16.71 ± 0.19
1996bo	0.016	15.65 ± 0.22
B		
SN	z	m_B^{eff}
1995ar	0.465	23.35 ± 0.22
1995as	0.498	23.74 ± 0.23
1995aw	0.400	22.57 ± 0.18
1995ax	0.615	23.38 ± 0.22
1995ay	0.480	22.90 ± 0.19
1995az	0.450	22.66 ± 0.20
1995ba	0.388	22.60 ± 0.18
1996cf	0.570	23.30 ± 0.18
1996cg	0.490	23.11 ± 0.18
1996ci	0.495	22.78 ± 0.18
1996cl	0.828	24.49 ± 0.46
1996cm	0.450	23.11 ± 0.18
1996cn	0.430	23.09 ± 0.19
1997F	0.580	23.57 ± 0.20
1997H	0.526	23.09 ± 0.19
1997I	0.172	20.29 ± 0.17
1997N	0.180	20.48 ± 0.17
1997O	0.374	23.60 ± 0.18
1997P	0.472	22.99 ± 0.18
1997Q	0.430	22.52 ± 0.17
1997R	0.657	23.80 ± 0.19
1997ac	0.320	21.96 ± 0.17
1997af	0.579	23.38 ± 0.18
1997ai	0.450	22.63 ± 0.22
1997aj	0.581	23.16 ± 0.18
1997am	0.416	22.63 ± 0.18
1997ap	0.830	24.38 ± 0.18

Table 1. (Continued.)

C		
SN	z	m_B^{eff}
1997ek	0.863	24.59 ± 0.19
1997eq	0.538	23.15 ± 0.18
1997ez	0.778	24.41 ± 0.18
1998as	0.355	22.66 ± 0.17
1998aw	0.440	23.26 ± 0.17
1998ax	0.497	23.47 ± 0.17
1998ay	0.638	23.92 ± 0.19
1998ba	0.430	22.90 ± 0.18
1998be	0.644	23.64 ± 0.18
1998bi	0.740	23.85 ± 0.17
2000fr	0.543	23.16 ± 0.17

The ΔE can be different from ΔE_e because of two effects. The first one is already studied in the previous section. The energy of light is proportional to its frequency and is less than the emitted energy ΔE_e by the redshift factor in (55). In other words, E is the zeroth component of the momentum 4-vector and transforms by the relation (27). The second effect is because the light gets fainter when propagated radially, usually known as the inverse square law. However, it is easier to find the combination of these two effects by the conservation of energy. To this end, we focus on the angular sector of the EM metric in spherical coordination $X^\mu = (cT, R, \theta, \varphi)$ and calculate the area of the surfaces of constant t and r, which is

$$\mathrm{d}s^2|_{t,r} = \frac{e^{\frac{2ct}{d}} r^2}{1 - \frac{r^2}{d^2}}(\mathrm{d}\theta^2 + \sin^2\theta \mathrm{d}\varphi^2) \quad \Rightarrow \quad A|_{t,r} = \frac{4\pi e^{\frac{2ct}{d}} r^2}{1 - \frac{r^2}{d^2}}. \tag{68}$$

Assuming that an spherical shell of light propagates outward from the origin at $r = 0$ and at the time $t = t_e$, by the conservation of energy the fall-off is proportional to the inverse of the area calculated at the observer's position, which is

$$\frac{1}{A_{\mathrm{O}}} = \frac{\left(1 - \frac{r^2}{d^2}\right)}{4\pi e^{\frac{2c(t_{\mathrm{O}} - t_e)}{d}} r^2}. \tag{69}$$

However, this fall-off is from the point of view of the sender. From the point of view of the receiver, the metric (and so, its angular sector) is re-scaled by the relation equation (32). Therefore, in the relation above the area is multiplied by a factor $e^{\frac{-2c(t_{\mathrm{O}} - t_e)}{d}}$, and hence,

$$\text{fall-off} \quad \propto \frac{1 - \frac{r^2}{d^2}}{r^2}. \tag{70}$$

The $\mathrm{d}\Omega$ can differ from $\mathrm{d}\Omega_e$ because of the aberration of the light rays. Similar to special relativity (see e.g., [92, 93]), the light of an isotropic source is more concentrated towards its direction of motion; that is called the headlight effect. To have self-contained paper, we derive this phenomenon step by step here. Consider a light ray that is emitted with an angle θ_e w.r.t the line of sight in figure 11 and into the solid angle $\mathrm{d}\Omega_e = \mathrm{d}\cos\theta_e \mathrm{d}\phi$. The ϕ is the azimuth around the line of sight, and the light ray is not going to be different in that direction. However, aberration changes the motion of the light ray in the θ direction as follows. Denoting the parallel and perpendicular speeds of the ray to the line of sight by $u_{e_\parallel} = c\cos\theta_e$ and $u_{e_\perp} = c\sin\theta_e$ respectively, we find

$$\tan\theta = \frac{u_\perp}{u_\parallel} = \frac{u_{e_\perp}}{\gamma(u_{e_\parallel} - \frac{cr}{d})} = \frac{\sin\theta_e}{\gamma(\cos\theta_e - \frac{r}{d})}, \tag{71}$$

in which the second equality is just replacement from equation (43). So,

$$\cos\theta = \frac{\cos\theta_e - \frac{r}{d}}{1 - \frac{r}{d}\cos\theta_e}. \tag{72}$$

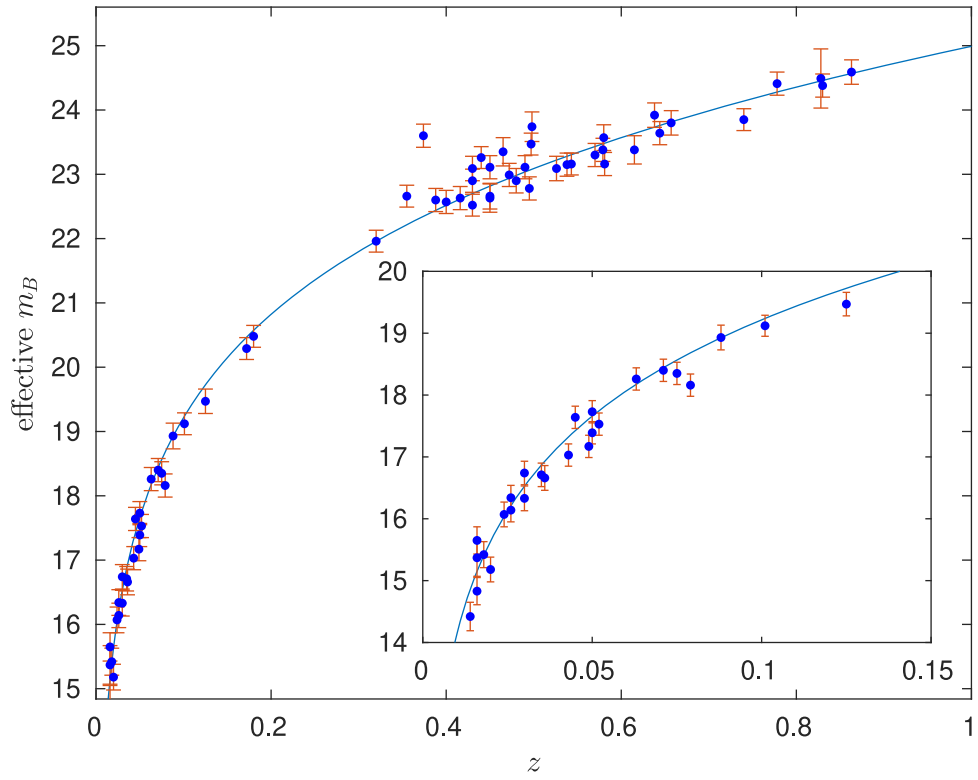

Figure 12. Hubble diagram in EM model: the blue dots and their error bars show the observed effective magnitude of 64 low and high redshift SNe Ia from Supernova Cosmology Project (SCP) [94] in terms of the redshift z. The curve is the plot of $m(z)$ that is fitted to the data, and yields $\mathcal{M} = 24.11 \pm 0.07$.

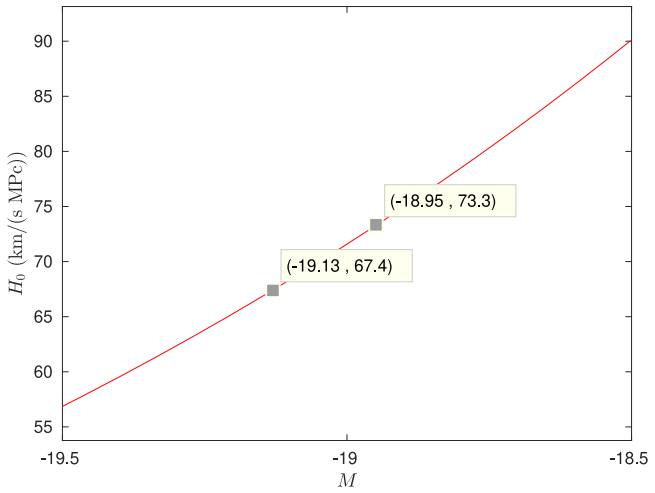

Figure 13. Hubble constant H_0 in terms of the SNe Ia absolute magnitude M resulted from the SCP data: the two points on the curve identify the values of M that reproduce the two discrepant values 67.4 and 73.3 $\text{kms}^{-1}\text{Mpc}^{-1}$ (among other reported values) that have resulted to the Hubble tension.

Taking a differentiation from both sides yields

$$\mathrm{d}\cos\theta = \frac{\mathrm{d}\cos\theta_e}{\gamma^2\left(1 - \frac{r}{d}\cos\theta_e\right)^2}. \tag{73}$$

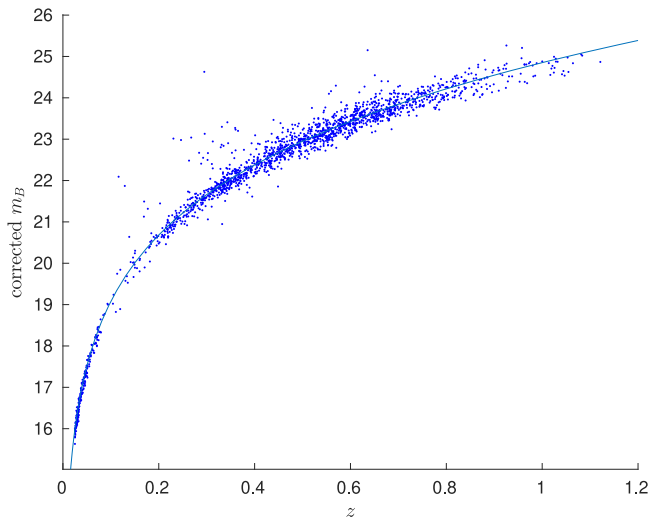

Figure 14. Hubble diagram in EM model: Corrected apparent magnitude versus redshift of 1829 SNe Ia (DES-5YR collaboration) are depicted by small blue dots. Error bars are not shown for a better visualization, while they are used in the curve-fitting procedure. The data of corrected magnitude as well as other interesting data such the errors are available in [101] based on the [8–14]. The curve is fitted resulting to $\mathcal{M} = 23.97 \pm 0.10$.

So, on the line of sight, that is $\theta_e = 0$ we find

$$\mathrm{d}\Omega = \frac{1+\frac{r}{d}}{1-\frac{r}{d}}\mathrm{d}\Omega_e. \tag{74}$$

Finally, by the first relation in equation (31) we find $\Delta t = \Delta t_e$. Collecting this equality with the previously achieved relations, that are the fall-off (70) and the aberration (74), we find

$$\frac{\Delta E}{\mathrm{d}\Omega\Delta t} = \frac{1-\frac{r^2}{d^2}}{r^2}\times\left(\frac{1+\frac{r}{d}}{1-\frac{r}{d}}\right)^{-1}\times\frac{\Delta E_e}{\mathrm{d}\Omega_e\Delta t_e} = \frac{\left(1-\frac{r}{d}\right)^2}{r^2}\times\frac{\Delta E_e}{\mathrm{d}\Omega_e\Delta t_e} = \frac{1}{d_L^2}\times\frac{\Delta E_e}{\mathrm{d}\Omega_e\Delta t_e}. \tag{75}$$

The last equation yields the promised relation (64). ■

7.3. Observational data and Hubble constant without tension

SNe type Ia are used as standard candles in distance measurements, because they have certain absolute magnitudes during their explosion. As a result, if we know their absolute magnitude at, e.g., the peak of the explosion, then we can find their luminosity distance by measuring their apparent magnitude via equation (60). However, the connection of the luminosity distance to the real distance is model-dependent. To resolve this issue, another piece of information, that is the redshift measurements, can help us to distinguish successful models of cosmology. In this section, we investigate the data of the effective apparent magnitude versus the observed redshift factor z for the SNe type Ia. For the ease of the reader, the data that we use is imported from [94] in table 1.

From the theoretical side, the apparent magnitude m as a function of z can be calculated by equations (60) and (65),

$$m(z) = \mathcal{M} + \log\left(\frac{z(z+2)}{2}\right), \tag{76}$$

in which

$$\mathcal{M} \equiv M + 5\log(\frac{c}{H_0}) + 25. \tag{77}$$

For the peak absolute magnitude M of SNe Ia, one can find a range of values from around -18.5 [52] to -19.5 [7], e.g., the values in [5, 33, 43, 54, 97–100]. However, as long as the curve fitting of the Hubble diagram is concerned, M and H_0 are not independent parameters. It is because in the curve fitting of the $m(z)$ with the data in Tab. 1, the combination of M and H_0 in the form of $\mathcal{M}$ enters into the calculation.

Using the nonlinear least-squares method to fit the curve equation (76) to the data in Tab. 1, we find $\mathcal{M} = 24.11 \pm 0.07$ with the remarkable 0.9915 R-square and adjusted R-square, 5.635 sum of squared errors and 95% confidence bound. figure 12 depicts the Hubble diagram of the data and the fitted curve of the effective

$m_B(z)$ (subscript B for Blue [94]). In the diagram, the blue dots and their error bars show the observed effective magnitude of 64 low and high redshift SNe Ia from Supernova Cosmology Project (SCP) [94] in terms of the redshift z. The curve depicts $m(z)$ that is fitted to the data, which yields the aforementioned value for the magnitude $\mathcal{M}$.

Replacing $\mathcal{M}$ into equation (77), the H_0 can be found in terms of M. The result is illustrated in figure 13. The horizontal axis in the diagram is the absolute magnitude M of SN Ia while the vertical axis depicts the Hubble constant H_0. It shows the sensitivity of the value of H_0 w.r.t the M. For example, the two values of H_0 that are reported from the Hubble Space Telescope data and the SH0ES Team in [48] and Planck CMB data[31, 56], i.e., 73.30 ± 1.04 and $67.4 \pm 0.5 \text{kms}^{-1}\text{Mpc}^{-1}$, can be derived in the EM model if we assume $M = -18.95 \pm 0.08$ and $M = -19.1 \pm 0.1$ respectively. As a result, the model is able to resolve the Hubble tension if the value of M is determined by local measurements to be around the latter value.

It is illuminating to compare and test the model with another data, the more recent Dark Energy Survey's five year (DES 5YR) SNe sample [8–14], that provides the corrected apparent magnitude m_B versus redshift z of the 1829 number of SNe Ia (see e.g., [101]). After repeating a similar curve fitting as above, we find the best fit $\mathcal{M} = 23.97 \pm 0.10$ with the 0.9843 R-square and adjusted R-square, 125.2 sum of squared errors and 95% confidence bound. The result is depicted in figure 14, where the horizontal and vertical axes are the redshift factor z and the corrected apparent magnitude m_B, respectively. Based on this set of data, the appropriate absolute magnitudes that reproduce the SH0ES and Planck reported Hubble constants are $M = -19.08 \pm 0.10$ and $M = -19.3 \pm 0.1$ respectively.

8. Discussion, outlook, and conclusion

Discussion

- EM is special relativity locally: Due to the unprecedented success of special relativity at local experiments, any model has to reduce to it locally. For the EM model, this happens when $\frac{ct}{d} \ll 1$ and $\frac{r}{d} \ll 1$. In other words, in the limit

$$\frac{ct}{d} \to 0 \qquad \text{and} \qquad \frac{r}{d} \to 0 \tag{78}$$

the special relativity is recovered. The easiest way to see it is to apply this limit to the EM metric (18), which results

$$e^{-\frac{ct}{d}} \to 1, \qquad f(r) \to 1, \tag{79}$$

and produces the standard metric (3) in the x^μ coordinates. Equivalently, one can use the coordinate relations (20) and find

$$\begin{pmatrix} cT \\ X \\ Y \\ Z \end{pmatrix} \to \begin{pmatrix} d + ct \\ x \\ y \\ z \end{pmatrix}, \tag{80}$$

while the d in the time component can be absorbed in the $\bar{X}^\mu$ convention that was discussed in section 2.2.1.

- Generators of infinitesimal EM transformations: The group structure of the EM transformations equation (39) is the Poincaré group, and so the infinite-dimensional representation of its algebra in terms of vector generators is the same as in the special relativity. For completeness, they are presented below:

$$\text{Change of EM frames: } H = \frac{1}{c}\partial_T, \quad P_i = \partial_{X^i}, \quad i \in \{1, 2, 3\}, \tag{81}$$

$$\text{Rotations: } J_{ij} = X^i\partial_{X^j} - X^j\partial_{X^i}, \tag{82}$$

$$\text{Translations (boosts): } C_i = \frac{1}{c}X^i\partial_T + cT\partial_{X^i} \tag{83}$$

with the commutation relations

$$\begin{aligned} &[H, C_i] = P_i, \qquad [P_i, C_j] = \delta_{ij}H, \qquad [J_{ij}, P_k] = \delta_{jk}P_i - \delta_{ik}P_j, \qquad [C_i, C_j] = J_{ij}, \\ &[J_{ij}J_{kl}] = \delta_{jk}J_{il} - \delta_{ik}J_{jl} + \delta_{il}J_{jk} - \delta_{jl}J_{ik}, \qquad [J_{ij}, C_k] = \delta_{jk}C_i - \delta_{ik}C_j. \end{aligned} \tag{84}$$

In the EM coordinates $x^\mu = (ct, x, y, z)$ the generators are

$$H = \sqrt{f}e^{-\frac{ct}{d}}\left(\frac{1}{fc}\partial_t - \frac{1}{d}x^i\partial_{x^i}\right), \; P_i = \sqrt{f}e^{-\frac{ct}{d}}\left(-\frac{x^i}{fcd}\partial_t + \partial_{x^i}\right), \tag{85}$$

$$J_{ij} = x^i\partial_{x^j} - x^j\partial_{x^i},\ C_i = fd\partial_{x^i} + \frac{x^ix^j}{d}\partial_{x^j}. \tag{86}$$

- Non-commutativity of the translations: From the previous argument, it can be seen that the EM translations C_i do not commute. The physical meaning of their commutation relation in equation (84) is that there is an extra rotation whenever we change the orders of translations in different directions. For example, if one moves forward to some distance and then moves leftward (notice that it is not turning to the left!) by another distance, she will be a bit rotated w.r.t another person who chooses to first move leftward and then forward.
- Rapidity and Farness: In special relativity, there is a dimensionless quantity that is called rapidity. It is defined by the relation $w_v = \tanh^{-1}(\beta)$ with $\beta = \frac{v}{c}$. It has the nice property that it follows the orthodox addition rule. For example, let us consider one spatial dimension for simplicity. If we transfer to a new inertial frame with the relative velocity v_1, and then, transfer to another one that has velocity v_2 in the new frame, then the overall procedure is not equivalent to transfer to an inertial frame with the velocity $v_1 + v_2$. However, the rapidity of the final frame w.r.t the initial frame is given by $w_1 + w_2$ correspondingly. An interesting feature of special relativity, that is not emphasized in the literature is that, in principle, we can measure the velocity of an object at least in two different ways: (I) using our rulers and synchronized clocks to find v directly; (II) changing our frame through small kicks, until we find the particle at rest in our last frame. In the second method and in the limit of infinitesimal kicks, if we sum up the number of kicks, we will find w_v instead of v itself. Note that in contrast with the v that is bounded above, w_v can take the values as large as one wishes. In analogy with the rapidity, we can define 'Farness' in the position. The definition of the farness is similar, but for positions

$$w_r \equiv \tanh^{-1}(\beta), \qquad \beta = \frac{r}{d}. \tag{87}$$

  Based on this definition, the previous argument on the different ways of measurement would make more sense; if we measure the distance to a galaxy by walking towards it and counting our steps, we would measure w_r instead of r or R. This is basically measuring the induced distances on our hyperboloid of constant time (see the metric (18)),

$$w_r = \frac{1}{d}\int_0^r \frac{\mathrm{d}r'}{f(r')}. \tag{88}$$

  The range of w_r is infinity, which means we can walk out of our Milky Way, taking infinite numbers of steps outward, and never reach the end of the Universe, any horizon, or any other special place.
- Horizon versus bound: The 'limiting length scale' (or 'bounded position') is a coordinate-dependent term, that is promoted to the similar status of special relativity's limiting speed. The more accurate terminology could be the 'cosmological horizon.' The EM model's horizon aligns with the de Sitter cosmological horizon because their causal structures are similar, a similarity rooted in the irrelevance of the conformal/Weyl factor in the metric (18)
- Geodesic equation: Although there is an extra scaling in the definition of the velocity in equation (34), the geodesic equation is satisfied by the straight lines in the Minkowski background. Explicitly, denoting $U^\mu \equiv e^{\frac{ct}{d}}U_0^\mu$ with a constant 4-vector U_0^μ (that generates straight lines by (12)),

$$U^\mu\nabla_\mu\ \ U^\nu = U^\mu\partial_\mu U^\nu = U^\mu\partial_\mu(e^{\frac{ct}{d}}U_0^\nu) = U_0^\nu U^\mu\partial_\mu e^{\frac{ct}{d}} = e^{\frac{ct}{d}}U_0^\nu U_0^\mu\partial_\mu e^{\frac{ct}{d}} = (U_0^\mu\partial_\mu e^{\frac{ct}{d}})U^\nu. \tag{89}$$

  The term in the last parenthesis is only a function of the proper time $\sigma = e^{\frac{ct}{d}}$, and so, this is the geodesic equation written in terms of a non-affine parameter.
- Unnecessary initial conditions: One of Milne's concerns in his model was to introduce the initial condition for the position and velocity of the matter at $T = 0$ such that it could lead to a linear recession of the galaxies (see sections III and IV of his book [68] for his comprehensive discussion). However, one can alternatively assume the cosmological principle, i.e., the homogeneity and isotropy of the matter density and its pressure on all maximally symmetric surfaces of constant time. This is what is done in section 6 by using equation (48). If it is not clear for the reader why such a matter content is homogeneous and isotropic on all of the EM hyperboloids, we encourage her or him to lower the index of $T^\mu{}_\nu$ by the dynamical form of the EM metric (22),

$$ds^2 = \frac{e^{\frac{2ct}{d}}}{f}\left[-fc^2dt^2 + a^2(t)\left(dx^2 + dy^2 + dz^2 + \frac{(xdx + ydy + zdz)^2}{d^2 f}\right)\right], \tag{90}$$

and then calculate the variation of the result by the Lie derivatives generated in the direction of vectors J_{ij} and C_i in (86). Vanishing outcome shows that $T_{\mu\nu}$ is invariant under the rotations and translations on hyperboloids; that means isotropy and homogeneity, respectively. In order to see how the cosmological principle yields the linear recession velocity of the matter, we can write down the $T_{\mu\nu}$ in the EM coordinates and compare it with the perfect fluid relation

$$T_{\mu\nu} = (\rho + P)W_\mu W_\nu + Pg_{\mu\nu}, \tag{91}$$

in which $W^\mu = \frac{dx^\mu}{d\sigma}$ is the EM velocity (not to be confused with the Cartesian U^μ in (34)). The result indicates $W^i = 0$, which shows that the matter is at rest w.r.t the EM coordinates (x, y, x), and so they follow the Hubble relation (44). As a result, we deduce that in the EM model, initial conditions are not necessary to be imposed on the matter.

- Flatness problem: One of the main supports of the spatially flat universe in ΛCDM model is the Hubble diagram of high redshift celestial objects. However, following back the dynamics of this model in time leads to a request for the fine-tuning of initial conditions of the model. This could be a challenge for the model if the inflation scenario could not be implemented. The problem is called 'flatness problem' in the literature. The reproduction of the Hubble diagram in the EM model was discussed extensively in the previous section, indicating that the data can be justified without assuming the flatness of the Universe. However, irrespective of this amendment, we note that the curvature of the EM hyperboloids (19) is inversely proportional to the d, and is different from Milne's equation (7)). So, if the constant d happens to have a very large value in comparison with the experimental distances, then the curvature could be negligible. This notation may resolve other possible experiments in favor of an approximately flat universe.
- Horizon problem: It is a mismatch between the observation and the ΛCDM model without inflation. The CMB data shows that different regions of the Universe, that in the standard model could never be in contact, are in thermal equilibrium with each other. This problem is called the 'horizon problem' and has been handled by the inflation proposal. In the EM model, the matter of the Universe has originated from the origin, $X^\mu = (0, 0, 0, 0)$. So, not only is the thermal equilibrium of very far regions in the sky not a problem, but it can also be considered as a confirmation for the model.
- Coordinate singularities: While the Milne metric exhibits coordinate singularities as $\tau \to 0$ and $\tau \to \infty$ (where metric components vanish or diverge), the EM metric (18) absorbs this feature into its conformal factor $e^{\frac{2ct}{d}}$. Instead, the EM metric introduces a new characteristic: a cosmological horizon at $r \to d$.
- More about $d_L(z)$: The EM relation between the luminosity distance and redshift in equation (65) is different from its analogue in the ΛCDM model (find it, e.g., in equation (7) of [7]). It is also different from the $d_L(z)$ in the Milne model (see [72, 74–76]) that has been falsified by the data.
- Milne's Hubble law: Combining the R_e in (66) with the EM Hubble's relations (44) and (45) reproduces Milne's version of the Hubble's law in equation (9).
- Two fundamental length scales: The Planck length scale ℓ_P is the length that can be derived from a combination of c, G, and $\hbar$, and is about 1.6×10^{-35} meters. The introduction of d as another fundamental length scale raises the question about the relation between these two different lengths. A possible answer could be that ℓ_P delimits the accessible distances from below, while d delimits the accessible distances from above. Based on the approximation $H_0 \approx 70 \text{kms}^{-1}\text{Mpc}^{-1}$, the d is roughly about 14 billion light years.
- Age of the Universe: In the EM model, all observers attribute the coordinate $(d, 0, 0, 0)$ to themselves, irrespective of what other observers measure about their position and time. So, it does not seem plausible to interpret $\frac{d}{c}$ as the age of the Universe, unless we would like to make ourselves privileged ones among other observers.
- What do we measure? The previous argument on the farness raises a question: which spatial distance do we measure in the lab? Is it R, r, or w_r? Or maybe other ones? The same question applies to the time direction. Do we measure T or t? The short answer may be: it depends on the setup of the experiment. Specially, the derivation of the $d_L(z)$ in the EM model and its agreement with observation may be suggestive that in the experiments of luminosity measurements, our clocks measure t, that is, the logarithm of the orthodox T. It sounds like a slogan that 'we measure the time logarithmically.'

Outlook

The curious reader may have noticed that there are many interesting subjects and questions that are skipped in this paper. Here are some of them, that the reader may add many to them. What physical implications has the horizon $r \to d$? What has happened at $T \to 0$? How do the CMB and its perturbations fit into the model? Can the direct observations related to the existence of the dark matter have a natural explanation in the EM model? How are other observations, such as the baryon acoustic oscillations and structure formation, explained by the model? What about other high-redshift observations such as quasars and gamma-ray bursts? Is the similarity of position and velocity related to the similarity of x and p in quantum mechanics and kinematics in the symplectic structures? What other implications may the scaling of time have? What could be the full and exact dynamic of the Universe in this model that reproduces the current density of observable matter? The topics are very attractive for further research, and any idea from the reader is welcomed. This work can be considered as an initial suggestion for deeper and more complete formulation of the relativistic model of the Universe. To enhance the analysis in this paper, future work will focus on the following key issues.

- It's essential to investigate the physical origin of the fundamental length scale d within the model.
- While the model fits supernova data, it's also expected to address other key cosmological observations, including Cosmic Microwave Background anisotropies, Baryon Acoustic Oscillations, and large-scale structure formation.
- Studying the dynamics of the metric in EM model a significant question that warrants dedicated research, and we're actively pursuing it; part of this work is already underway and will appear in a forthcoming paper.
- Future work will compare and discuss cosmological models beyond ΛCDM and EM to provide a comprehensive overview of the context.

Conclusion

In the Einstein-Milne model, an observer attributes the coordinate $X^\mu = (d, 0, 0, 0)$ and the 4-velocity $U^\mu = (c, 0, 0, 0)$ to herself. The invariant constants d and c are the maximum position and velocity in the model. The shifts in Poincaré group change the frames, while the Lorentz subgroup (augmented by scaling) does the job of transformation within a frame. In the model, homogeneity and isotropy of matter yield the Hubble recession in the Universe. This recession via the Doppler effect results in the cosmological redshift and the observed Hubble diagrams. In this model, there is no need for dark matter and energy, as well as acceleration, to handle the observed data. Moreover, the Hubble tension can be released if the absolute magnitude of SNe Ia is fixed by local observations. The model suggests that the space and time that we measure depend on the setup of the experiment. Especially, the clocks may measure the logarithm of the Cartesian time in special relativity.

Acknowledgments

I am thankful to Jutta Kunz for her supports, and Farshad Abdollahnia for fruitful discussions.

Data availability statement

All data that support the findings of this study are included within the article (and any supplementary files).

References

[1] Hubble E 1929 A relation between distance and radial velocity among extra-galactic nebulae *Proc. Nat. Acad. Sci.* **15** 168–73
[2] Perlmutter S *et al* (Supernova Cosmology Project Collaboration) 1999 Measurements of Omega and Lambda from 42 high redshift supernovae *Astrophys. J.* **517** 565–86
[3] Riess A G *et al* (Supernova Search Team) 1998 Observational evidence from supernovae for an accelerating universe and a cosmological constant *Astron. J.* **116** 1009
[4] Hamuy M 1993 The 1990 Calan/Tololo Supernova Search *Astron. J* **106** IOP 2392
[5] Hamuy M, Phillips M M, Schommer R A, Suntzeff N B, Maza J and Aviles R 1996 The absolute luminosities of the Calan/Tololo type IA supernovae *Astron. J.* **112** 2391
[6] Hamuy M, Phillips M M, Suntzeff N B, Schommer R A, Maza J and Aviles R 1996 The Hubble diagram of the Calan/Tololo type IA supernovae and the value of HO *Astron. J.* **112** 2398
[7] Perlmutter S and Schmidt B P 2003 Measuring cosmology with supernovae *Lect. Notes Phys.* **598** 195–217
[8] Abbott T M C *et al* (DES) 2024 The dark energy survey: cosmology results with 1500 new high-redshift type Ia supernovae using the full 5 yr data set *Astrophys. J. Lett.* **973** L14
[9] Vincenzi M *et al* (DES) 2024 The dark energy survey supernova program: cosmological analysis and systematic uncertainties *Astrophys. J.* **975** 86

[10] Sánchez B O *et al* (DES) 2024 The dark energy survey supernova program: light curves and 5 Yr data release *Astrophys. J.* **975** 5
[11] Möller A *et al* (DES) 2024 The dark energy survey 5-yr photometrically classified type Ia supernovae without host-galaxy redshifts *Mon. Not. Roy. Astron. Soc.* **533** 2073–88
[12] Lee J *et al* (DES) 2023 The dark energy survey supernova program: corrections on photometry due to wavelength-dependent atmospheric effects *Astron. J.* **165** 222
[13] Kelsey L *et al* (DES) 2022 Concerning colour: the effect of environment on type Ia supernova colour in the dark energy survey *Mon. Not. Roy. Astron. Soc.* **519** 3046–63
[14] Wiseman P *et al* (DES) 2020 Supernova host galaxies in the dark energy survey: I. deep coadds, photometry, and stellar masses *Mon. Not. Roy. Astron. Soc.* **495** 4040–60
[15] Hicken M, Challis P, Jha S, Kirsher R P, Matheson T, Modjaz M, Rest A and Wood-Vasey W M 2009 CfA3: 185 Type Ia supernova light curves from the CfA *Astrophys. J.* **700** 331–57
[16] Hicken M *et al* 2012 CfA4: light curves for 94 Type Ia supernovae *Astrophys. J. Suppl.* **200** 12
[17] Chen P *et al* 2022 The first data release of CNIa0.02-A complete nearby (Redshift <0.02) sample of type Ia supernova light curves* *Astrophys. J. Supp.* **259** 53
[18] Krisciunas K *et al* 2017 The carnegie supernova project I: third photometry data release of low-redshift type Ia supernovae and other white dwarf explosions *Astron. J.* **154** 211
[19] Brown P J, Breeveld A A, Holland S, Kuin P and Pritchard T 2014 SOUSA: the swift optical/ultraviolet supernova archive *Astrophys. Space Sci.* **354** 89
[20] Scolnic D M *et al* (Pan-STARRS1) 2018 The complete light-curve sample of spectroscopically confirmed SNe Ia from Pan-STARRS1 and cosmological constraints from the combined pantheon sample *Astrophys. J.* **859** 101
[21] Sako M *et al* (SDSS) 2008 The sloan digital sky survey-II supernova survey: search algorithm and follow-up observations *Astron. J.* **135** 348–73
[22] Stahl B E *et al* 2019 Lick observatory supernova search follow-up program: photometry data release of 93 type Ia supernovae *Mon. Not. Roy. Astron. Soc.* **490** 3882–907
[23] Brout D *et al* 2022 The pantheon+ analysis: cosmological constraints *Astrophys. J.* **938** 110
[24] Scolnic D *et al* 2022 The pantheon+ analysis: the full data set and light-curve release *Astrophys. J.* **938** 113
[25] Carroll S M 2001 The cosmological constant *Living Rev. Rel.* **4**
[26] Peebles P J E 1984 Tests of Cosmological Models Constrained by Inflation *Astrophys. J.* **284** 439–44
[27] Peebles P J E and Ratra B 2003 The cosmological constant and dark energy *Rev. Mod. Phys.* **75** 559–606
[28] Einstein A 1917 Kosmologische Betrachtungen zur allgemeinen Relativitätstheorie *Sitzungsberichte der Königlich Preußischen Akademie der Wissenschaften (Berlin)* **6** 142–52
[29] Bertone G and Hooper D 2018 History of dark matter *Rev. Mod. Phys.* **90** 045002
[30] de Swart J, Bertone G and van Dongen J 2017 How dark matter came to matter *Nature Astron* **1** 0059
[31] Aghanim N *et al* (Planck) 2020 Planck 2018 results. VI. cosmological parameters *Astron. Astrophys.* **641** A6 erratum: Astron. Astrophys. 652, C4 (2021)
[32] Weinberg D H, Mortonson M J, Eisenstein D J, Hirata C, Riess A G and Rozo E 2013 Observational probes of cosmic acceleration *Phys. Rept.* **530** 87–255
[33] Perivolaropoulos L and Skara F 2022 Challenges for ΛCDM: an update *New Astron. Rev.* **95** 101659
[34] Bull P *et al* 2016 Beyond ΛCDM: problems, solutions, and the road ahead *Phys. Dark Univ.* **12** 56–99
[35] Abdalla E *et al* 2022 Cosmology intertwined: a review of the particle physics, astrophysics, and cosmology associated with the cosmological tensions and anomalies *JHEAp* **34** 49–211
[36] Risaliti G and Lusso E 2019 Cosmological constraints from the Hubble diagram of quasars at high redshifts *Nature Astron* **3** 272–7
[37] Demianski M, Piedipalumbo E, Sawant D and Amati L 2017 Cosmology with gamma-ray bursts: I. the Hubble diagram through the calibrated $E_{p,i}$ - E_{iso} correlation *Astron. Astrophys.* **598** A112
[38] Liu Y, Liang N, Xie X, Yuan Z, Yu H and Wu P 2022 Gamma-ray burst constraints on cosmological models from the improved amati correlation *Astrophys. J.* **935** 7
[39] Lusso E, Piedipalumbo E, Risaliti G, Paolillo M, Bisogni S, Nardini E and Amati L 2019 Tension with the flat ΛCDM model from a high-redshift Hubble diagram of supernovae, quasars, and gamma-ray bursts *Astron. Astrophys.* **628** L4
[40] Colgáin E. Ó., Sheikh-Jabbari M M and Yin L 2025 Do high redshift QSOs and GRBs corroborate JWST? *Physics of the Dark Universe* **49** 101975
[41] E. Ó. Colgáin, Sheikh-Jabbari M M, Solomon R, Dainotti M G and Stojkovic 2024 Putting flat ΛCDM in the (Redshift) bin *Phys. Dark Univ.* **44** 101464
[42] Colgáin E. Ó., Sheikh-Jabbari M M and Solomon R 2023 High redshift ΛCDM cosmology: to bin or not to bin? *Phys. Dark Univ.* **40** 101216
[43] Malekjani M, Conville R M, Ó. Colgáin E, Pourojaghi S and Sheikh-Jabbari M M 2024 On redshift evolution and negative dark energy density in pantheon + supernovae *Eur. Phys. J. C* **84** 317
[44] Adil S A, Akarsu Ö., Malekjani M, Colgáin E. Ó., Pourojaghi S, Sen A A and Sheikh-Jabbari M M 2023 S8 increases with effective redshift in ΛCDM cosmology *Mon. Not. Roy. Astron. Soc.* **528** L20–6
[45] Akarsu Ö., Ó. Colgáin E, Sen A A and Sheikh-Jabbari M M 2024 ΛCDM tensions: localising missing physics through consistency checks *Universe* **10** 305
[46] Colgáin E. Ó., Dainotti M G, Capozziello S, Pourojaghi S, Sheikh-Jabbari M M and Stojkovic D Does DESI 2024 Confirm ΛCDM arXiv:2404.08633
[47] Colgáin E. Ó., Pourojaghi S and Sheikh-Jabbari M M 2025 Implications of DES 5YR SNe Dataset for ΛCDM *Eur. Phys. J. C* **85** 3
[48] Riess A G *et al* 2022 A comprehensive measurement of the local value of the Hubble constant with 1 km s^{-1}Mpc^{-1} uncertainty from the Hubble space telescope and the SH0ES team *Astrophys. J. Lett.* **934** L7
[49] Riess A G *et al* 2016 A 2.4% determination of the local value of the hubble constant *Astrophys. J.* **826** 56
[50] Cardona W, Kunz M and Pettorino V 2017 Determining H_0 with Bayesian hyper-parameters *JCAP* 056
[51] Feeney S M, Mortlock D J and Dalmasso N 2018 Clarifying the Hubble constant tension with a Bayesian hierarchical model of the local distance ladder *Mon. Not. Roy. Astron. Soc.* **476** 3861–82
[52] Dhawan S, Jha S W and Leibundgut B 2018 Measuring the Hubble constant with Type Ia supernovae as near-infrared standard candles *Astron. Astrophys.* **609** A72
[53] Burns C R *et al* (CSP) 2018 The carnegie supernova project: absolute calibration and the Hubble constant *Astrophys. J.* **869** 56
[54] Camarena D and Marra V 2020 Local determination of the Hubble constant and the deceleration parameter *Phys. Rev. Res.* **2** 013028

[55] Riess A G, Yuan W, Casertano S, Macri L M and Scolnic D 2020 The accuracy of the Hubble constant measurement verified through cepheid amplitudes *Astrophys. J. Lett.* **896** L43
[56] Ade P A R *et al* (Planck) 2016 Planck 2015 results. XIII. cosmological parameters *Astron. Astrophys.* **594** A13
[57] Pogosian L, Zhao G B and Jedamzik K 2020 Recombination-independent determination of the sound horizon and the Hubble constant from BAO *Astrophys. J. Lett.* **904** L17
[58] Balkenhol L *et al* (SPT-3G) 2021 Constraints on ΛCDM extensions from the SPT-3G 2018 EE and TE power spectra *Phys. Rev. D* **104** 083509
[59] Alam S *et al* (eBOSS) 2021 Completed SDSS-IV extended baryon oscillation spectroscopic survey: cosmological implications from two decades of spectroscopic surveys at the apache point observatory *Phys. Rev. D* **103** 083533
[60] Philcox O H E and Ivanov M M 2022 BOSS DR12 full-shape cosmology: ΛCDM constraints from the large-scale galaxy power spectrum and bispectrum monopole *Phys. Rev. D* **105** 043517
[61] Aiola S *et al* (ACT) 2020 The atacama cosmology telescope: DR4 maps and cosmological parameters *JCAP* **12** 047
[62] Freedman W L 2017 Cosmology at a crossroads *Nature Astron* **1** 0121
[63] Di Valentino E, Mena O, Pan S, Visinelli L, Yang W, Melchiorri A, Mota D F, Riess A G and Silk J 2021 In the realm of the Hubble tension-a review of solutions *Class. Quant. Grav.* **38** no 153001
[64] Blanchard A, Héloret J Y, Ilić S, Lamine B and Tutusaus I 2024 ΛCDM is alive and well *Open J. Astrophys.* **7** 117170
[65] Freedman W L, Madore B F, Jang I S, Hoyt T J, Lee A J and Owens K A 2025 Status Report on the Chicago-Carnegie Hubble Program (CCHP): Measurement of the Hubble Constant Using the Hubble and James Webb Space Telescopes *Astrophys. J.* **985** 203
[66] Knox L and Millea M 2020 Hubble constant hunter's guide *Phys. Rev. D* **101** 043533
[67] Lopez-Corredoira M and Marmet L 2022 Alternative ideas in cosmology *Int. J. Mod. Phys. D* **31** 2230014
[68] Milne E A 1933 World-structure and the expansion of the universe *Z. Astrophysik* **6** 1–35
[69] Milne E A 1935 Relativity, gravitation and world structure(Oxford University Press)
[70] Milne E A 1948 *Kinematic relativity: a sequel to relativity, gravitation, and world structure* (Oxford University Press)
[71] Wigner E P 2001 Review of 'kinematic relativity: a sequel to relativity, gravitation, and world structure' ed J Mehra Historical and Biographical Reflections and Syntheses *Historical and Biographical Reflections and Syntheses. Historical, Philosophical, and Socio-Political Papers, vol B/7* (Springer)
[72] Macleod A 2005 An Interpretation of Milne cosmology arXiv:physics/0510170
[73] Cannon J W *et al* 1997 *Hyperbolic Geometry, Flavors of Geometry* **31** 2
[74] Dev A, Sethi M and Lohiya D 2001 Linear coasting in cosmology and sne ia *Phys. Lett. B* **504** 207
[75] Davis T M and Lineweaver C H 2004 Expanding confusion: common misconceptions of cosmological horizons and the superluminal expansion of the universe *Publ. Astron. Soc. Austral.* **21** 97
[76] Chodorowski M J 2005 Cosmology under Milne's shadow *Publ. Astron. Soc. Austral.* **22** 287
[77] Benoit-Levy A and Chardin G Observational constraints of a Milne Universe arXiv:0811.2149
[78] Krishnan C and Roy S 2014 Desingularization of the Milne universe *Phys. Lett. B* **734** 92–5
[79] Ling E Milne-like Spacetimes and their Symmetries arXiv:1803.00174
[80] Benoit-Levy A and Chardin G 2012 Introducing the Dirac-Milne universe *Astron. Astrophys.* **537** A78
[81] Chardin G and Manfredi G 2018 Gravity, antimatter and the Dirac-Milne universe *Hyperfine interact* **239** 45
[82] Klinkhamer F R and Ling E Model for a time-symmetric Milne-like universe without big bang curvature singularity arXiv:1909.05816
[83] Saharian A A and Petrosyan T A 2020 The Casimir densities for a sphere in the Milne universe *Symmetry* **12** 619
[84] Manfredi G, Rouet J L, Miller B N and Chardin G 2020 Structure formation in a Dirac-Milne universe: comparison with the standard cosmological model *Phys. Rev. D* **102** 103518
[85] Lewis G F and Barnes L A 2021 The one-way speed of light and the Milne universe *Publ. Astron. Soc. Austral.* **38** e007
[86] Ling E and Ling E 2022 Remarks on the cosmological constant appearing as an initial condition for Milne-like spacetimes *Gen. Rel. Grav* **54** 68 [erratum: Gen. Rel. Grav. 54, no.11, 139 (2022)]
[87] Ling E and Piubello A 2023 On the asymptotic assumptions for Milne-like spacetimes *Gen. Rel. Grav.* **55** 53
[88] Wang J and Yuan W 2025 Global stability of the open Milne spacetime *Annales Henri Poincare* **26** 2467–2504
[89] Vishwakarma R G 2020 Resolving Hubble tension with the Milne model *Int. J. Mod. Phys. D* **29** 2043025
[90] Zenginoğlu A. 2024 Hyperbolic times in Minkowski space *Am. J. Phys.* **92** 965
[91] Sitnikov L S 2006 Hubble's law and superluminity recession velocities arXiv:astro-ph/0602102
[92] Rybick G B and Lightman A P 1985 *Radiative Processes in Astrophysics* (Wiley-Interscience)
[93] Ghisellini G 2013 Radiative processes in high energy astrophysics *Lect. Notes Phys.* **873** 1–147
[94] Knop R A *et al* (Supernova Cosmology Project) 2003 New constraints on Omega(M), Omega(lambda), and w from an independent set of eleven high-redshift supernovae observed with HST *Astrophys. J.* **598** 102
[95] Hamuy M 1996 BVRI light curves for 29 type IA supernovae *Astron. J* **112** IOP 2408
[96] Riess A G *et al* 1999 BV RI light curves for 22 type Ia supernovae *Astron. J.* **117** 707–24
[97] Branch D and Miller D L 1993 Type IA supernovae as standard candles *Astrophys. J.* **405** IOP L5
[98] Hillebrandt W and Niemeyer J C 2000 Type Ia supernova explosion models *Ann. Rev. Astron. Astrophys.* **38** 191–230
[99] Camarena D and Marra V 2020 A new method to build the (inverse) distance ladder *Mon. Not. Roy. Astron. Soc.* **495** 2630–44
[100] Camarena D and Marra V 2021 On the use of the local prior on the absolute magnitude of Type Ia supernovae in cosmological inference *Mon. Not. Roy. Astron. Soc.* **504** 5164–71
[101] 2025 https://github.com/des-science/DES-SN5YR